High-Oxidation-State Pentamethylcyclopentadienyl Tungsten Hydrazine and Hydrazido Complexes and Cleavage of the N-N Bond

Richard R. Schrock,* Timothy E. Glassman, Michael G. Vale, and Moshe Kol

Contribution from the Department of Chemistry 6-331, Massachusetts Institute of Technology, Cambridge, Massachusetts 02139. *Received September 3, 1992*

Abstract: $[Cp^*WMe_3(\eta^2\text{-}NH_2NH_2)][OTf]$ (**1a**), which is prepared by adding hydrazine to $Cp^*WMe_3(OTf)$, is a pseudooctahedral complex in which the N(1)-N(2) bond distance is 1.43(1) Å. Deprotonation of **1a** is proposed to yield unobserved $Cp^*WMe_3(NHNH_2)$, which disproportionates to a mixture of 0.5 equiv of $Cp^*WMe_3(\eta^1\text{-}NNH_2)$, 0.5 equiv of $Cp^*WMe_3(NH)$, and 0.5 equiv of ammonia. The proposed intermediates in the disproportionation reaction are $Cp^*WMe_3(\eta^2\text{-}NNH_2)$ and $Cp^*WMe_3(\eta^2\text{-}NH_2NH_2)$. The instability of $Cp^*WMe_3(\eta^2\text{-}NH_2NH_2)$ toward N-N bond cleavage is suggested by the reduction of $[Cp^*WMe_3(\eta^2\text{-}NH_2NH_2)]^+$ to give a 1:1 mixture of $Cp^*WMe_3(NH)$ and ammonia. Addition of 1,2-dimethylhydrazine to $Cp^*WMe_3(OTf)$ in ether yields red crystalline $[Cp^*WMe_3(\eta^2\text{-}NHMeNHMe)][OTf]$ (**1b**), which upon deprotonation yields a mixture of 0.5 equiv of $Cp^*WMe_3(\eta^2\text{-}MeNNMe)$ and 0.5 equiv of $Cp^*WMe_3(NMe)$ via (it is proposed) disproportionation of $Cp^*WMe_3(NMeNHMe)$. Deprotonation of $[Cp^*WMe_3(\eta^2\text{-}NMeNHMe)]^+$ yields $Cp^*WMe_3(\eta^2\text{-}MeNNMe)$ quantitatively. An X-ray structure of $Cp^*WMe_3(\eta^2\text{-}MeNNMe)$ revealed that the dimethyldiazene ligand is bound to the metal in the expected η^2 manner but that the nitrogen atom that is sp^2-hybridized is located approximately in a basal position of a square pyramid, while the sp^3-hybridized nitrogen atom occupies a position above what is roughly the plane formed by the three methyl carbon atoms and N(1), a result that is consistent with roughly equal abilities of the $\pi_\parallel$ and $\pi_\perp$ orbitals in the Cp^*WMe_3 fragment to form a metal-ligand π bond. $Cp^*WMe_3(\eta^2\text{-}MeNNMe)$ decomposes to $Cp^*WMe_3(NMe)$ in solution in high yield at 60 °C, is not readily reduced by sodium amalgam, is protonated by triflic acid to give $[Cp^*WMe_3(\eta^2\text{-}NMeNHMe)][OTf]$, and is alkylated by methyl triflate to give $[Cp^*WMe_3(\eta^2\text{-}NMeNMe_2)][OTf]$. Addition of 1,2-diphenylhydrazine to $Cp^*WMe_3(OTf)$ in ether did not yield $[Cp^*WMe_3(\eta^2\text{-}NHPhNHPh)][OTf]$ (**1c**), but it did yield a mixture of anilinium triflate, $[Cp^*WMe_3(\eta^2\text{-}NPhNHPh)][OTf]$ (**4c**), and $Cp^*WMe_3(NPh)$ over a period of 24 h. Sodium hydride in THF will deprotonate **4c** to give $Cp^*WMe_3(\eta^2\text{-}PhNNPh)$ (**5c**) in 94% yield. Reduction of **4c** by either Na/Hg or cobaltocene led to $Cp^*WMe_3(NPh)$, **5c**, and $PhNH_2$. Although **5c** was stable at 65 °C in C_6D_6 for 4 days, it was reduced by sodium amalgam in C_6D_6 to give $Cp^*WMe_3(NPh)$ in ca. 65% yield in 16 h. Addition of methylhydrazine to $Cp^*WMe_3(OTf)$ gave $[Cp^*WMe_3(\eta^2\text{-}NH_2NHMe)][OTf]$ (**1d**) quantitatively. Deprotonation of **1d** with DBU in THF results in the formation of equal parts of $Cp^*WMe_3(\eta^1\text{-}NNHMe)$, $Cp^*WMe_3(NH)$, and methylamine. The reaction between **1d** and NEt_3 in dichloromethane cleanly generates $Cp^*WMe_3(\eta^1\text{-}NNHMe)$ in high yield along with dihydrogen. Reduction of **1d** in THF yields a mixture of $Cp^*WMe_3(NH)$, $Cp^*WMe_3(NMe)$, and $Cp^*WMe_3(\eta^1\text{-}NNHMe)$. Addition of NH_2NMe_2 to $Cp^*WMe_3(OTf)$ in ether at -40 °C yields impure $[Cp^*WMe_3(NH_2NMe_2)][OTf]$ (**1e**). Deprotonation of **1e** by either NEt_3 or DBU in THF or dichloromethane is proposed to yield $Cp^*WMe_3(NHNMe_2)$ (**2e**), which then disproportionates to yield a mixture of $Cp^*WMe_3(NH)$, dimethylamine, and $Cp^*WMe_3(NNMe_2)$. Reduction of **1e** with Na/Hg in ether or sodium naphthalenide in THF yields $Cp^*WMe_3(NH)$ and $NHMe_2$, the expected products of N-N bond cleavage in $Cp^*WMe_3(\eta^2\text{-}NH_2NMe_2)$ (**3e**). Reduction of $[Cp^*WMe_3(\eta^2\text{-}NH_2NH_2)]^+$ or $Cp^*WMe_3(\eta^1\text{-}NNH_2)$ in the presence of a proton source yields up to 92% of the possible ammonia, while up to 10 equiv of added hydrazine can be reduced catalytically under similar conditions to yield between 72 and 98% ammonia. It is proposed that the N-N bond is cleaved in $Cp^*WMe_3(\eta^x\text{-}NH_2NH_2)$ (x = 1 or 2) to give ammonia and $Cp^*WMe_3(NH)$ in these reductions.

Introduction

For the last two decades inorganic chemists have been trying to determine how dinitrogen might be reduced to ammonia at a transition-metal center,[1-3] a process that presumably is the key to reduction of dinitrogen by various nitrogenase enzymes that contain iron (always) and molybdenum (most commonly) or vanadium.[2-12] Although coordination of dinitrogen to transition-metal centers is no longer rare, many dinitrogen complexes can be protonated to give $M{=}NNH_2$ species,[1,3,13-18] and cleavage of the N-N bond has been observed in many Mo and W complexes,[1,3,19-24] reports in the literature of the catalytic reduction of dinitrogen by transition-metal complexes are rare[25-28] and in

(1) Chatt, J.; Dilworth, J. R.; Richards, R. L. *Chem. Rev.* **1978**, *78*, 589.
(2) Henderson, R. A.; Leigh, G. J.; Pickett, C. J. *Adv. Inorg. Chem. Radiochem.* **1983**, *27*, 197.
(3) Leigh, G. J. *J. Mol. Catal.* **1988**, *47*, 363.
(4) Hawkes, T. R.; McLean, P. A.; Smith, B. E. *Biochem. J.* **1984**, *217*, 317.
(5) *Advances in Nitrogen Fixation Research*; Veeger, C., Newton, W. E., Eds.; Dr. W. Junk/Martinus Nijhoff: Boston, 1984.
(6) Orme-Johnson, W. H. *Ann. Rev. Biophys. Chem.* **1985**, *14*, 419.
(7) Joerger, R. D.; Premakumar, R.; Bishop, P. E. *J. Bacteriol.* **1986**, *16B*, 673.
(8) Morningstar, J. E.; Hales, B. J. *J. Am. Chem. Soc.* **1987**, *109*, 6854.
(9) Eady, R. R.; Robson, R. L.; Richardson, T. H.; Miller, R. W.; Hawkins, M. *Biochem. J.* **1987**, *244*, 297.
(10) Hales, B. J.; Case, E. E. *J. Biol. Chem.* **1987**, *282*, 16205.
(11) Conradson, S. D.; Burgess, B. K.; Newton, W. E.; Mortenson, L. E.; Hodgson, K. O. *J. Am. Chem. Soc.* **1987**, *109*, 7507.
(12) Burgess, B. *Chem. Rev.* **1990**, *90*, 1377.
(13) Henderson, R. A. *J. Chem. Soc., Dalton Trans.* **1982**, 917.
(14) George, T. A.; Ma, L.; Shjailh, S. N.; Tisdale, R. C.; Zubieta, J. *Inorg. Chem.* **1990**, *29*, 4789.
(15) George, T. A.; Tisdale, R. C. *Polyhedron* **1989**, *8*, 1756.
(16) George, T. A.; Koczon, L. M.; Tisdale, R. C.; Gebreyes, K.; Ma, L.; Shaikh, S.; Zubieta, J. *Polyhedron* **1990**, *9*, 545.
(17) Chatt, J.; Pearman, A. J.; Richards, R. L. *J. Chem. Soc., Dalton Trans.* **1978**, 1766.
(18) Anderson, S. A.; Fakley, M. E.; Richards, R. L.; Chatt, J. *J. Chem. Soc., Dalton Trans.* **1981**, 1973.
(19) Baumann, J. A.; Bossard, G. E.; George, T. A.; Howell, D. B.; Koczon, L. M.; Lester, R. K.; Noddings, C. M. *Inorg. Chem.* **1985**, *24*, 3568.
(20) Henderson, R. A.; Leigh, G. J.; Pickett, C. J. *J. Chem. Soc., Dalton Trans.* **1989**, 425.
(21) Hussain, W.; Leigh, G. J.; Pickett, C. J. *J. Chem. Soc., Chem. Commun.* **1982**, 747.
(22) George, T. A.; Tisdale, R. C. *Inorg. Chem.* **1988**, *27*, 2909.
(23) Takahashi, T.; Mizobe, Y.; Sato, M.; Uchida, Y.; Hidai, M. *J. Am. Chem. Soc.* **1980**, *102*, 7461.
(24) Lazarowych, N. J.; Morris, R. H.; Ressner, J. M. *Inorg. Chem.* **1986**, *25*, 3926.
(25) Dickson, C. R.; Nozik, A. J. *J. Am. Chem. Soc.* **1978**, *100*, 8007.
(26) Yu, M.; Didenko, L. P.; Kachapina, L. M.; Shilov, A. E.; Shilova, A. K.; Struchkov, Y. T. *J. Chem. Soc., Chem. Commun.* **1989**, 1467.
(27) Dziegielewski, J. O.; Grzybek, R. *Polyhedron* **1990**, *9*, 645.
(28) Shilov, A. E. *J. Mol. Catal.* **1987**, *41*, 221.

0002-7863/93/1515-1760$04.00/0

Table I. Bond Distances and Angles in $[Cp^*WMe_3(\eta^2\text{-}NH_2NH_2)][OTf]$ (**1a**)

	Bond Distances (Å)		
W–N(1)	2.131(7)	W–C(4)	2.370(8)
W–N(2)	2.174(7)	W–C(5)	2.366(8)
N(1)–N(2)	1.43(1)	W–C(6)	2.348(8)
W–C(1)	2.20(1)	W–C(7)	2.340(8)
W–C(2)	2.173(9)	W–C(8)	2.379(8)
W–C(3)	2.21(2)		
	Bond Angles (deg)		
N(1)–W–N(2)	38.3(3)	N(2)–W–C(2)	93.2(3)
W–N(2)–N(1)	69.0(4)	N(2)–W–C(3)	74.4(3)
W–N(1)–N(2)	72.2(4)	N(1)–W–C(1)	83.5(3)
Cp–W–N(2)	157.0	N(1)–W–C(2)	132.0(3)
N(2)–W–C(1)	73.2(3)	N(1)–W–C(3)	83.0(3)

no case has the catalytically active transition-metal complex been identified or the mechanism elucidated. It also is rare to find a system in which ammonia is generated exclusively (no hydrazine) or one in which ammonia is generated by addition of electrons from an external source.[29–32] Inorganic dinitrogen chemistry and N–N bond cleavage studies have been dominated by chemistry that begins with Mo(0) or W(0) dinitrogen phosphine complexes ("low-oxidation-state" dinitrogen chemistry).[1]

In the last few years we have been exploring the chemistry of N_2H_x ligands in monoCp* tungsten and molybdenum complexes in which the metal is in a relatively high oxidation state (4+, 5+, or 6+). $[Cp^*WMe_3]_2(\mu\text{-}N_2)$ can be prepared in high yield by reducing $Cp^*WMe_3(OTf)$ ($Cp^* = \eta^5\text{-}C_5Me_5$, $OTf = OSO_2CF_3$) in the presence of dinitrogen,[33] which is good evidence that a metal in a relative high oxidation state (probably d^2 in this case) can bind dinitrogen. Many monomeric N_2H_x species ($x = 2$–4) that contain the Cp^*WMe_3 core also are now known, examples being $[Cp^*WMe_3(\eta^2\text{-}NHNH_2)]^+$[34] and $[Cp^*WMe_3(\eta^2\text{-}NH_2NH_2)]^+$.[35] Complexes containing NH_y ligands that are possible intermediates in a reduction cycle involving complexes having the Cp^*WMe_3 core also have been isolated, e.g., $Cp^*WMe_3(NH)$, $Cp^*WMe_3(NH_2)$, and $[Cp^*WMe_3(NH_3)_x]^+$ ($x = 1$ or 2).[36] Most importantly, ammonia is produced in high yield when monomeric Cp^*WMe_3 species in which the N–N bond is still present are reduced in the presence of protons.[35] We also have discovered that hydrazine can be reduced catalytically to ammonia under similar conditions.[35] Analogous Mo complexes have been prepared and employed to reduce hydrazine catalytically in yields comparable to the analogous W complexes, but in general the analogous chemistry of molybdenum has been more difficult to control and elucidate.

In this paper we report studies aimed at elucidating the chemistry of tungsten complexes in which N–N bond cleavage occurs, in particular W(IV) hydrazine and W(V) hydrazido complexes. Reactions in which the N–N bond is cleaved by reduction in the presence of protons also are discussed. Related molybdenum chemistry will be published separately. Some of these results have been reported in a preliminary fashion.[35,37]

Results

Synthesis and Reactivity of $[Cp^*WMe_3(NH_2NH_2)]^+$. Several years ago we discovered that $Cp^*WMe_3(OTf)$ reacts with hydrazine to give a paramagnetic orange adduct that we proposed to be $[Cp^*WMe_3(\eta^2\text{-}NH_2NH_2)][OTf]$ (**1a**, eq 1).[38] An X-ray

$$Cp^*WMe_3(OTf) \underset{+\,HOTf\,-\,[N_2H_5][OTf]}{\overset{NH_2NH_2}{\rightleftharpoons}} \underset{\mathbf{1a}}{[Cp^*WMe_3(\eta^2\text{-}NH_2NH_2)][OTf]} \qquad (1)$$

structure of **1a** (Figure 1, Table I) now confirms that proposal. The ligands adopt a pseudooctahedral geometry similar to that found in $[Cp^*WMe_3(\eta^2\text{-}NHNH_2)][OTf]$.[34] Three orbitals are available for bonding in a Cp^*WMe_3 core of this type:[39] a σ orbital pointing toward the fourth square pyramidal position and two π orbitals, a $\pi_\parallel$ orbital (ca. 65% d_{xy}) and a $\pi_\perp$ orbital (ca. 50% d_{z^2}).[40] (The z axis is coincident with the W–Cp* axis; the $\pi_\parallel$ orbital lies approximately parallel to the Cp* ligand and extends between the "equatorial" ligands.) In $[Cp^*WMe_3(\eta^2\text{-}NHNH_2)][OTf]$ the "equatorial" W–N(1) distance (1.86(1) Å) suggests that an sp^2-hybridized nitrogen atom is doubly bonded to the metal through the $\pi_\parallel$ orbital while the "axial" W–N(2) distance (2.15(1) Å) is consistent with it being a single (dative) bond to one lobe of the $\pi_\perp$ orbital. In **1a** the "equatorial" W–N(1) bond (2.131(7) Å) is only slightly shorter than the "axial" W–N(2) bond (2.174(7) Å), consistent with both being dative single bonds. The slightly longer W–N(2) bonds in **1a** presumably results from poorer overlap of the N(2) lone pair with the $\pi_\perp$ orbital, which in part may result from the relatively small N(1)–W–N(2) bite angle (38.3(3)°). The N(1)–N(2) distance (1.43(1) Å) is consistent with an N–N single bond[41] and is slightly longer than the 1.39(1) Å found in $[Cp^*WMe_3(\eta^2\text{-}NHNH_2)][OTf]$. The metal achieves a 17-electron count in **1a** when the N_2H_4 ligand is bound in an η^2 fashion, and we presume on the basis of the X-ray structure that the single electron in **1a** resides in the nonbonding $\pi_\parallel$ orbital.

The IR spectrum of **1a** shows absorptions for the asymmetric and symmetric NH_2 stretching modes between 3350 and 3050

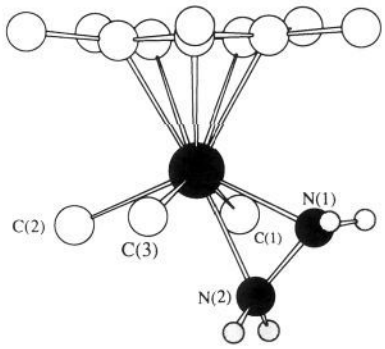

Figure 1. Drawing of the structure of $[WCp^*Me_3(\eta^2\text{-}NH_2NH_2)][OTf]$ (**1a**; anion omitted).

Scheme I

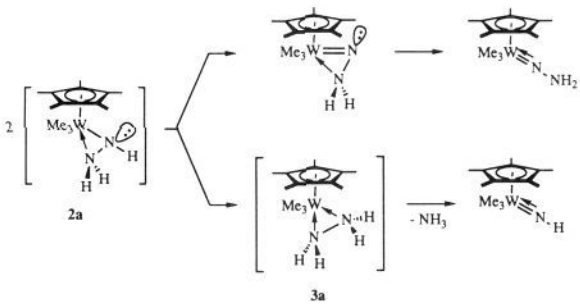

(29) George, T. A.; Kaul, B. B. *Inorg. Chem.* **1990**, *29*, 4969.
(30) George, T. A.; Kaul, B. B. *Inorg. Chem.* **1991**, *30*, 882.
(31) Pickett, C. J.; Talarmin, J. *Nature* **1985**, *317*, 652.
(32) Pickett, C. J.; Ryder, K. S.; Talarmin, J. *J. Chem. Soc., Dalton Trans.* **1986**, 1453.
(33) O'Regan, M. B.; Liu, A. H.; Finch, W. C.; Schrock, R. R.; Davis, W. M. *J. Am. Chem. Soc.* **1990**, *112*, 4331.
(34) Schrock, R. R.; Liu, A. H.; O'Regan, M. B.; Finch, W. C.; Payack, J. F. *Inorg. Chem.* **1988**, *27*, 3574.
(35) Schrock, R. R.; Glassman, T. E.; Vale, M. G. *J. Am. Chem. Soc.* **1991**, *113*, 725.
(36) Glassman, T. E.; Vale, M. G.; Schrock, R. R. *Organometallics* **1991**, *10*, 4046.
(37) Glassman, T. E.; Vale, M. G.; Schrock, R. R. *Inorg. Chem.* **1992**, *31*, 1985.
(38) Liu, A. H. Ph.D. Thesis, Massachusetts Institute of Technology, 1988.
(39) Kubacek, P.; Hoffmann, R.; Havlas, Z. *Organometallics* **1982**, *1*, 180.
(40) Extended Hückel calculations on a CAChe system using the Cp^*WMe_3 core geometry from the X-ray structure of $[Cp^*WMe_3(\eta^2\text{-}NHNH_2)][OTf]$ revealed the following contributions (of >10%) to the three orbitals: $\pi_\parallel$, d_{xy} (65%), $d_{x^2-y^2}$ (12%), d_{xz} (14%); $\pi_\perp$, d_{z^2} (48%), $d_{x^2-y^2}$ (17%), d_{yz} (13%); σ, d_{yz} (32%), d_{z^2} (17%), $d_{x^2-y^2}$ (15%), s (12%). We thank C. C. Cummins for these calculations.
(41) *Tables of Interatomic Distances and Configuration in Molecules and Ions*; Sutton, L. E., Ed.; Chemical Society, Special Publication 11; The Chemical Society: London, 1958.

Table II. Products of Deprotonating W(V) Hydrazine Adducts

complex	base	solvent	products	ratio	yield
$[Cp^*WMe_3(\eta^2\text{-}NH_2NH_2)]^+$ (**1a**)	NEt_3	CH_2Cl_2	$Cp^*WMe_3(NH)$	29	82
			$Cp^*WMe_3(\eta^1\text{-}NNH_2)$	17	
			$[Cp^*WMe_3]_2(\mu\text{-}N_2)$[a]	54	
1a	DBU	THF or CH_2Cl_2	$Cp^*WMe_3(NH)$	50	88
			$Cp^*WMe_3(\eta^1\text{-}NNH_2)$	49	
$[Cp^*WMe_3(\eta^2\text{-}NHMeNHMe)]^+$ (**1b**)	DBU	THF	$Cp^*WMe_3(NMe)$	59	73
			$Cp^*WMe_3(\eta^2\text{-}MeNNMe)$	37	
$[Cp^*WMe_3(\eta^2\text{-}NH_2NHMe)]^+$ (**1d**)	NEt_3	CH_2Cl_2	$Cp^*WMe_3(\eta^1\text{-}NNMeH)$		77
1d	DBU	THF	$Cp^*WMe_3(NH)$	48	72
			$Cp^*WMe_3(\eta^1\text{-}NNMeH)$	52	
$[Cp^*WMe_3(\eta^2\text{-}NH_2NMe_2)]^+$ (**1e**)	NEt_3 or DBU	CH_2Cl_2	$Cp^*WMe_3(NH)$	27	74
			$Cp^*WMe_3(\eta^1\text{-}NNMe_2)$	73	
1e	NEt_3 or DBU	THF	$Cp^*WMe_3(NH)$	48	72[b]
			$Cp^*WMe_3(\eta^1\text{-}NNMe_2)$	18	

[a] Only a trace observed in THF. [b] A small amount of $Cp^*WMe_3(O)$ is observed in most reactions as a consequence of the presence of traces of water.

cm^{-1} and for the NH_2 bending modes between 1640 and 1590 cm^{-1}, similar to the IR spectrum of $[Cp^*WMe_4(\eta^2\text{-}NH_2NH_2)]^+$[34] and to IR spectra of analogous hydrazine adducts described later. The ESR spectrum of **1a** is similar to those of analogous tungsten(V) ammonia and amide complexes;[36] one broad absorption is found near $\langle g \rangle = 2.00$. Solution conductivities of **1a** are consistent with it being a 1:1 electrolyte.

Addition of triflic acid to **1a** produces $Cp^*WMe_3(OTf)$ and $[N_2H_5][OTf]$ quantitatively. This result is not surprising since $[Cp^*WMe_3(NH_3)_x]^+$ complexes (x = 1 or 2) also react readily with triflic acid to form $Cp^*WMe_3(OTf)$ and $[NH_4][OTf]$.[36] Evidently one end of the hydrazine ligand in **1a** dissociates in solution, and therefore hydrazine can be protonated and lost from the coordination sphere.

A solution of **1a** in THF slowly decomposes to form a mixture of $Cp^*WMe_3(\eta^1\text{-}NNH_2)$[34,42] and $Cp^*WMe_3(NH)$.[36] Since **1a** reacts with triflic acid, we propose that it decomposes via bimolecular proton transfer to produce $Cp^*WMe_3(OTf)$, $[N_2H_5][OTf]$, and an unobserved $Cp^*WMe_3(NHNH_2)$ complex (**2a**). As we shall discuss below, **2a** can be produced in other reactions and appears to disproportionate to $Cp^*WMe_3(\eta^1\text{-}NNH_2)$ and unobserved $Cp^*WMe_3(NH_2NH_2)$ (**3a**); **3a** is proposed to undergo N–N bond cleavage to give $Cp^*WMe_3(NH)$ and ammonia (see Scheme I and later Discussion). Such reactions are potentially complex for two reasons: the presence of protons raises the possibility of proton-catalyzed reactions and intermolecular reactions involving proton transfer are usually rapid. $Cp^*WMe_3(NHNH_2)$ (**2a**) is a 17-electron species if the hydrazido ligand is bound as a three-electron donor (counting covalently bound $NHNH_2$ as a radical). In structure **2a**-η^1 the unpaired electron occupies the $\pi_\perp$ orbital, while in structure **2a**-η^2 it occupies the $\pi_\parallel$ orbital. What the actual structure is may have a major impact on the reaction pathways available to $Cp^*WMe_3(NHNH_2)$, as we shall see.

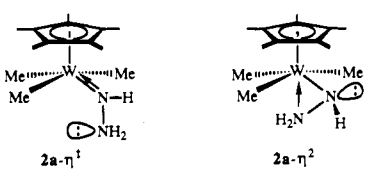

We believe that **2a** is generated in situ upon deprotonating **1a** with DBU in THF or dichloromethane (eq 2); **2a** subsequently

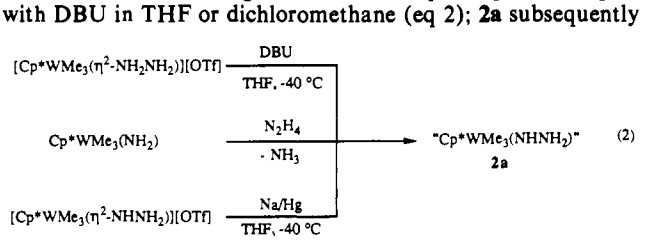

(2)

decomposes to give a mixture of $Cp^*WMe_3(NH)$ (and ammonia) and $Cp^*WMe_3(\eta^1\text{-}NNH_2)$ (Table II). In one experiment the reaction was monitored at low temperature by ^1H NMR after triethylamine was added to **1a** at −80 °C in CD_2Cl_2. The initial stages of the reaction were difficult to follow due to the presence of paramagnetic species. However, at −40 °C, $Cp^*WMe_3(NH)$ and $Cp^*WMe_3(\eta^2\text{-}NNH_2)$[42] were observed when the reaction was approximately half finished. ($Cp^*WMe_3(\eta^2\text{-}NNH_2)$ has been prepared at low temperature; its structure was proposed on the basis of ^{15}N NMR studies.[42]) Intermediate $Cp^*WMe_3(\eta^2\text{-}NNH_2)$ isomerized to $Cp^*WMe_3(\eta^1\text{-}NNH_2)$ upon warming the reaction mixture to room temperature. The ratio of $Cp^*WMe_3(NH)$ to the total $Cp^*WMe_3(\eta^2\text{-}NNH_2)$ and $Cp^*WMe_3(\eta^1\text{-}NNH_2)$ was 1:1 throughout the reaction. The resonance for ammonia was broadened into the base line due to rapid proton exchange with $[NEt_3H][OTf]$. Deprotonation of **1a** with NEt_3 in dichloromethane at room temperature resulted in the formation of $[Cp^*WMe_3]_2(\mu\text{-}N_2)$ as the major product (Table II), $Cp^*WMe_3(NH)$ and $Cp^*WMe_3(\eta^1\text{-}NNH_2)$ being minor products. Since $[Cp^*WMe_3(\eta^2\text{-}NHNH_2)][OTf]$ is known to react with $Cp^*WMe_3(\eta^1\text{-}NNH_2)$ or $Cp^*WMe_3(NH)$ to form $[Cp^*WMe_3]_2(\mu\text{-}N_2)$,[42] we believe that only a strong base can completely deprotonate **1a** before **1a** can react with products that contain basic nitrogen sites to give $[Cp^*WMe_3]_2(\mu\text{-}N_2)$. Therefore, only reactions employing DBU yield $Cp^*WMe_3(NH)$ and $Cp^*WMe_3(\eta^1\text{-}NNH_2)$ cleanly and in high yield.

Reduction of $[Cp^*WMe_3(\eta^2\text{-}NHNH_2)]^+$ with sodium amalgam in THF at −40 °C is also believed to yield **2a** (eq 2), since $Cp^*WMe_3(\eta^1\text{-}NNH_2)$ and $Cp^*WMe_3(NH)$ again are the metal-containing products (Table IV), although they are not formed as cleanly and in equal amounts. $[Cp^*WMe_3]_2(\mu\text{-}N_2)$ again is formed in approximately 30% relative yield as a result of complex redox and acid/base chemistry. Use of sodium naphthalenide (a homogeneous reductant) in THF at −40 °C produced a 1:2 mixture of $Cp^*WMe_3(NH)$ and $Cp^*WMe_3(\eta^1\text{-}NNH_2)$, no $[Cp^*WMe_3]_2(\mu\text{-}N_2)$ being observed.

The third method of generating **2a** consisted of adding hydrazine to $Cp^*WMe_3(NH_2)$[36] in THF at 25 °C (eq 2); a 1:1 mixture of $Cp^*WMe_3(\eta^1\text{-}NNH_2)$ and $Cp^*WMe_3(NH)$ (87% total yield) was produced. This reaction is one of the proposed steps in the cycle discussed later in which hydrazine is catalytically reduced to ammonia. An important feature of the reaction between $Cp^*WMe_3(NH_2)$ and N_2H_4, in contrast to the other two reactions shown in eq 2, is that no cationic complexes (relatively good proton sources) or electron sources (other than W complexes) are present. Therefore, it is perhaps important to note that this reaction gives $Cp^*WMe_3(\eta^1\text{-}NNH_2)$ and $Cp^*WMe_3(NH)$ in the highest yield. This result suggests that $Cp^*WMe_3(NHNH_2)$ could disproportionate to $Cp^*WMe_3(\eta^1\text{-}NNH_2)$ and unstable $Cp^*WMe_3(NH_2NH_2)$, and $Cp^*WMe_3(NH_2NH_2)$ could then decompose to $Cp^*WMe_3(NH)$ and ammonia, all in the absence of protons and electrons. (See Discussion later.) It also suggests that $[Cp^*WMe_3]_2(\mu\text{-}N_2)$ is indeed formed in a side reaction.

A proposed method of disproportionation of **2a** in the absence

(42) Glassman, T. E.; Vale, M. G.; Schrock, R. R. *J. Am. Chem. Soc.* **1992**, *114*, 8098.

Table III. Products of Reducing Cationic W(V) Hydrazine Adducts[a]

complex	reducing agent	products	ratio	yield
$[Cp^*WMe_3(\eta^2\text{-}NH_2NH_2)]^+$ (**1a**)	Na/Hg[b]	$Cp^*WMe_3(NH)$	78	78
		$[Cp^*WMe_3]_2(\mu\text{-}N_2)$	22	
1a	$Na(C_{10}H_8)$	$Cp^*WMe_3(NH)$	69	69
		$[Cp^*WMe_3]_2(\mu\text{-}N_2)$	31	
$[Cp^*WMe_3(\eta^2\text{-}NHMeNHMe)]^+$ (**1b**)	Na/Hg	$Cp^*WMe_3(NMe)$	57	63
		$Cp^*WMe_3(\eta^2\text{-}MeNNMe)$	18	
		$[Cp^*WMe_3(\eta^2\text{-}NMeNHMe)]^+$	25	
1b	$Na(C_{10}H_8)$	$Cp^*WMe_3(NMe)$		65
$[Cp^*WMe_3(\eta^2\text{-}NH_2NHMe)]^+$ (**1d**)	Na/Hg[b]	$Cp^*WMe_3(NH)$	50	67[c,d]
		$Cp^*WMe_3(\eta^1\text{-}NNMeH)$	49	
1d	Na/Hg	$Cp^*WMe_3(NH)$	24	72[c]
		$Cp^*WMe_3(NMe)$	23	
		$Cp^*WMe_3(\eta^1\text{-}NNHMe)$	46	
1d	$Na(C_{10}H_8)$	$Cp^*WMe_3(NH)$	52	70
		$Cp^*WMe_3(NMe)$	5	
		$Cp^*WMe_3(\eta^1\text{-}NNHMe)$	43	
$[Cp^*WMe_3(\eta^2\text{-}NH_2NMe_2)]^+$ (**1e**)	Na/Hg[b]	$Cp^*WMe_3(NH)$	68	87
		$Cp^*WMe_3(\eta^1\text{-}NNMe_2)$	32	
1e	$Na(C_{10}H_8)$	$Cp^*WMe_3(NH)$	60	70[c]
		$Cp^*WMe_3(\eta^1\text{-}NNMe_2)$	21	

[a] Reaction done in THF unless otherwise noted. [b] Reaction done in ether. [c] $WCp^*Me_3(O)$ present as a side product as a consequence of the presence of traces of water. [d] $WCp^*Me_3(NMe)$ present in trace amounts.

Table IV. Products of Reducing Cationic W(VI) Hydrazido(1–) Complexes[a]

complex	reducing agent	products	ratio	yield
$[Cp^*WMe_3(\eta^2\text{-}NHNH_2)]^+$ (**4a**)	Na/Hg	$Cp^*WMe_3(NH)$	27	75
		$Cp^*WMe_3(\eta^1\text{-}NNH_2)$	41	
		$[Cp^*WMe_3]_2(\mu\text{-}N_2)$	32	
4a	$Na(C_{10}H_8)$ (−40 °C)	$Cp^*WMe_3(NH)$	32	72
		$Cp^*WMe_3(\eta^1\text{-}NNH_2)$	68	
$[Cp^*WMe_3(\eta^2\text{-}NMeNHMe)]^+$ (**4b**)	Na/Hg	$Cp^*WMe_3(NMe)$		80
$[Cp^*WMe_3(\eta^2\text{-}NPhNHPh)]^+$ (**4c**)	Na/Hg	$Cp^*WMe_3(NPh)$	70	
		$Cp^*WMe_3(\eta^2\text{-}PhNNPh)$	30	
4c	$CoCp_2$	$Cp^*WMe_3(NPh)$	55	
		$Cp^*WMe_3(\eta^2\text{-}PhNNPh)$	45	
$[Cp^*WMe_3(\eta^2\text{-}NMeNH_2)]^+$ (**4d**)	Na/Hg	$Cp^*WMe_3(NH)$	8	78
		$Cp^*WMe_3(NMe)$	6	
		$Cp^*WMe_3(\eta^1\text{-}NNMeH)$	86	
4d	$Na(C_{10}H_8)$	$Cp^*WMe_3(NH)$	4	74
		$Cp^*WMe_3(NMe)$	3	
		$Cp^*WMe_3(\eta^1\text{-}NNMeH)$	93	

[a] Solvent = THF unless otherwise noted.

of an acid is shown in Scheme I. (This and other possibilities are discussed in more detail later.) The observation of intermediate $Cp^*WMe_3(\eta^2\text{-}NNH_2)$ when **1a** is deprotonated at low temperature is good evidence that an α hydrogen atom is removed from **2a** in a bimolecular reaction to form **3a**. We could test the proposal that $Cp^*WMe_3(NH_2NH_2)$ (**3a**) is an unstable intermediate in the disproportionation of **2a** and a precursor to $Cp^*WMe_3(NH)$ and ammonia by reducing $[Cp^*WMe_3(\eta^2\text{-}NH_2NH_2)][OTf]$ (**1a**) with sodium amalgam in ether at −40 °C. $Cp^*WMe_3(NH)$ and ammonia (Table III) are formed in moderate yield, but $[Cp^*WMe_3]_2(\mu\text{-}N_2)$, which we propose results from secondary acid/base and redox chemistry, is also formed in ca. 20% absolute yield. Use of sodium naphthalenide in THF did not prevent formation of $[Cp^*WMe_3]_2(\mu\text{-}N_2)$. Since **1a** is also a potential proton source in the reaction shown in eq 3, we can conclude from

$$\underset{\mathbf{1a}}{[Cp^*WMe_3(\eta^2\text{-}NH_2NH_2)][OTf]} \xrightarrow[-\ NaOTf]{Na/Hg} Cp^*WMe_3(NH) + NH_3 \qquad (3)$$

these data alone only that "$Cp^*WMe_3(\eta^2\text{-}NH_2NH_2)$" decomposes to $Cp^*WMe_3(NH)$ and ammonia in the presence of a potential proton source. As we noted above, **2a** disproportionates cleanly when it is prepared by adding hydrazine to $Cp^*WMe_3(NH_2)$. Therefore, the N–N bond in "$Cp^*WMe_3(\eta^2\text{-}NH_2NH_2)$" could be cleaved efficiently in the absence or presence of protons.

Cyclic voltammetry studies of **1a** (employing a 0.1 M solution of $[NBu_4][BF_4]$ in dichloromethane) revealed a reduction wave at −0.65 V, but only approximately 30% of the reduction product (on the basis of the ratio of cathodic to anodic currents) is oxidized back to **1a** in the oxidation cycle (200 mV/s sweep rate). The time required to reoxidize the reduced species under these conditions is approximately 15 s. If we assume that **1a** is reduced by only one electron in the reduction process, then the reduced species is likely to be "$Cp^*WMe_3(NH_2NH_2)$", and it is decomposing to a significant extent in a period of approximate 15 s.

Reactions Involving 1,2-Dimethylhydrazine. Addition of 1,2-dimethylhydrazine to $Cp^*WMe_3(OTf)$ in ether yields red crystalline $[Cp^*WMe_3(\eta^2\text{-}NHMeNHMe)][OTf]$ (**1b**). We propose that 1,2-dimethylhydrazine in **1b** binds to the metal center in an η^2 fashion, as found for hydrazine in **1a** in the solid state. The IR spectrum of **1b** lacks the absorptions characteristic of NH_2 stretching and bending modes, as one would expect. **1b** appears to be significantly more stable in solution than **1a**; a bimolecular protonation/deprotonation reaction, the proposed mode of (slow) decomposition of **1a**, should be slower for **1b** for steric reasons.

$[Cp^*WMe_3(\eta^2\text{-}NHMeNHMe)][OTf]$ can be deprotonated by DBU or NEt_3 to yield a mixture of a diazene complex, $Cp^*WMe_3(\eta^2\text{-}MeNNMe)$ (**5b**), $Cp^*WMe_3(NMe)$,[36] and methylamine (eq 4). Typically, more $Cp^*WMe_3(NMe)$ is formed

$$\underset{\mathbf{1b}}{2\,[Cp^*WMe_3(\eta^2\text{-}NHMeNHMe)][OTf]} \xrightarrow[-\ 2\,[DBUH][OTf]]{2\ DBU} Cp^*WMe_3(\eta^2\text{-}MeNNMe)\ (\mathbf{5b}) + Cp^*WMe_3(NMe) + Me_2NH \qquad (4)$$

than **5b** (Table II), probably because **5b** decomposes slowly to $Cp^*WMe_3(NMe)$ (see below). We propose that $Cp^*WMe_3(\eta^2\text{-}NMeNHMe)$ (**2b**) is the product of deprotonating **1b** and that **2b** disproportionates via a bimolecular transfer of H·. However,

Scheme II

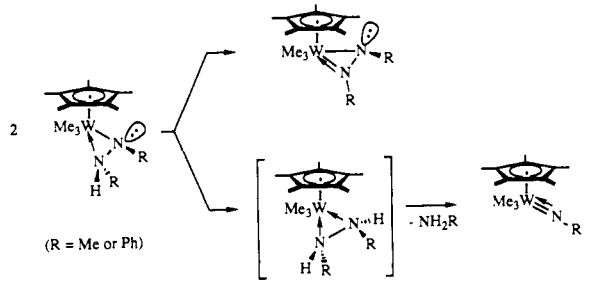

H• can be abstracted only from the sp^3-hybridized N_β in **2b** (Scheme II), in contrast to the reaction shown in Scheme I where H• can be abstracted from the sp^2-hybridized N_α in **2a**. Therefore, $Cp^*WMe_3(\eta^2$-MeNNMe) (**5b**) is formed (which cannot rearrange to $Cp^*WMe_3(\eta^1$-$NNMe_2)$, a known compound[42]) along with intermediate $Cp^*WMe_3(\eta^2$-NMeHNMeH) (**3b**). Cleavage of the N–N bond in **3b** then yields methylamine and Cp^*WMe_3(NMe) (Scheme II). Again, these data do not tell us whether protons are required for N–N bond cleavage under these conditions.

Compound **5b** can be prepared most readily by the sequence of reactions shown in eq 5. $[Cp^*WMe_4(\eta^2$-NHMeNHMe)][PF_6],

$$[Cp^*WMe_4][PF_6] \xrightarrow[-\,CH_4]{MeNHNHMe} [Cp^*WMe_3(\eta^2\text{-}NMeNHMe)][PF_6]\ \mathbf{4b}\text{-}PF_6 \xrightarrow[-\,CH_4]{MeMgCl} \mathbf{5b} \quad (5)$$

which most likely is formed when 1,2-dimethylhydrazine adds to $[Cp^*WMe_4][PF_6]$,[42] evidently is unstable toward loss of methane. Deprotonation of **4b** with methyl magnesium chloride yields **5b** in high yield; weaker bases such as triethylamine do *not* deprotonate **4b**. This fact stands in contrast to the finding that $[Cp^*WMe_3(\eta^2$-$NHNH_2)][OTf]$ is deprotonated by DBU or triethylamine to yield $Cp^*WMe_3(\eta^2$-$NNH_2)$ at low temperature, which rearranges to $Cp^*WMe_3(\eta^1$-$NNH_2)$ in a first-order manner.[42] The fact that a strong base (MeMgCl) is required to form **5b** suggests that it is more difficult to remove H_β than H_α in general in W(VI) hydrazido(1–) complexes of this type, although steric factors may also play a role. It does not seem as likely that $[Cp^*WMe_3(\eta^2$-$NHNH_2)]^+$ is deprotonated at N_β to form intermediate $Cp^*WMe_3(\eta^2$-HNNH), which then rearranges to $Cp^*WMe_3(\eta^1$-$NNH_2)$, although that possibility cannot be discounted at this stage. (Rearrangement of an η^2 diazene ligand to an η^1 hydrazido(2–) ligand would be analogous to rearrangement of an η^2 acetylene complex to an η^1 vinylidene complex.[43]) $[Cp^*WMe_3(\eta^2$-NMeNHMe)][OTf] (**4b**-OTf), which is obtained by adding 1 equiv of triflic acid to **5b** at low temperature, behaves entirely analogously to **4b**-PF_6 in deprotonation reactions.

On the basis of the X-ray structure of $[Cp^*WMe_3(\eta^2$-$NHNH_2)][OTf]$, we expected that the $\pi_\parallel$ orbital in **5b** would be employed to form the dative π bond. However, an X-ray study of **5b** (Figure 2, Table V) revealed that although the dimethyldiazene ligand is bound to the metal in the expected η^2 manner, the nitrogen atom that is sp^2-hybridized (sum of angles around N(1) = 350.5°) is located approximately in a basal position of a square pyramid, while the sp^3-hybridized nitrogen atom (sum of angles around N(2) = 297°) occupies a position above what is roughly the plane formed by the three methyl carbon atoms and N(1). Evidently the $\pi_\perp$ orbital is used to form the dative π bond (W–N(1) = 1.860(8) Å), while the dative σ bond between N(2) and the metal (W–N(2) = 2.126(7) Å) involves the $\pi_\parallel$ orbital. These data suggest that the $\pi_\parallel$ and $\pi_\perp$ orbitals in the Cp^*WMe_3 fragment are roughly equivalent in their ability to form a metal–ligand π bond. The N(1)–N(2) bond length (1.38(1) Å) is considerably lengthened compared to that found for dimethyldiazene itself (1.254(3) Å)[44] and approximately the same as N–N bond lengths found in $Ni(t$-$BuNC)_2(\eta^2$-PhNNPh) (1.385(5) Å),[45] $Ni[P(tolyl)_3]_2(\eta^2$-PhNNPh) (1.371(6) Å),[46] Ti-

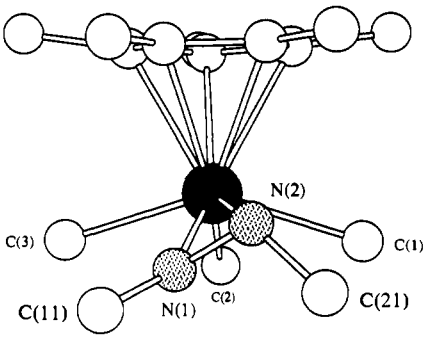

Figure 2. Drawing of the structure of $WCp^*Me_3(\eta^2$-MeNNMe) (**5b**).

Table V. Selected Bond Distances and Bond Angles in $WCp^*Me_3(\eta^2$-MeNNMe) (**5b**)

Bond Distances (Å)			
W–N(1)	1.860(8)	W–C(3)	2.205(9)
W–N(2)	2.126(7)	N(1)–N(2)	1.38(1)
W–C(1)	2.212(8)	N(1)–C(11)	1.46(1)
W–C(2)	2.225(9)	N(1)–C(21)	1.48(1)
Bond Angles (deg)			
N(1)–W–N(2)	39.7(3)	N(2)–W–C(2)	137.8(3)
N(1)–W–C(1)	102.3(4)	N(2)–W–C(3)	114.2(3)
N(1)–W–C(2)	116.0(4)	W–N(1)–N(2)	80.6(5)
N(1)–W–C(3)	76.2(4)	W–N(1)–C(11)	151.7(7)
C(1)–W–C(2)	71.0(4)	N(2)–N(1)–C(11)	118.2(8)
C(1)–W–C(3)	137.8(4)	W–N(2)–N(1)	59.7(4)
C(2)–W–C(3)	72.2(4)	W–N(2)–C(21)	126.5(6)
N(2)–W–C(1)	81.5(3)	N(1)–N(2)–C(21)	110.8(8)

$(\eta^5$-$C_5H_5)_2(\eta^2$-PhNNPh) (1.339(8) Å),[47] $Sm(\eta^5$-$C_5Me_5)_2(\eta^2$-PhNNPh)(THF) (1.388(15) or 1.323(14) Å),[48] and Ti(O-2,6-C_6H_5-i-$Pr_2)_2$(py)$_2(\eta^2$-PhNNPh) (1.416(8) Å),[49] consistent with a considerable amount of reduction to a $(\eta^2$-MeNNMe)$^{2-}$ ligand. To our knowledge, there is no other example of a monometallic complex containing any η^2-RNNR ligand where R is not Ph.

The proton NMR spectrum of **5b** in THF-d_8 at room temperature reveals a broad resonance at 3.01 ppm for the methyl groups of the dimethyldiazene ligand. At −80 °C, two dimethyldiazene methyl resonances are observed at δ H 2.70 and 3.17 (δ C 38.59 and 40.16), $\Delta G^\ddagger$ for equilibration being 13.6 kcal/mol at 5 °C. These data are consistent with a fluxional process that interconverts the two NMe groups in an intermediate having a mirror plane in which the $\pi_\perp$ orbital is nonbonding (see below; methyl ligands omitted). Equilibration of the two ends of the dimethyldiazene ligand via complete dissociation of it from the metal seems much less likely in view of the electron-deficient nature (14 electrons) of the resulting Cp^*WMe_3 core.

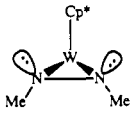

$Cp^*WMe_3(\eta^2$-MeNNMe) decomposes slowly at room temperature in solution to form Cp^*WMe_3(NMe), which can be isolated in 85–90% overall yield after several days. Decomposition of **5b** in C_6D_6 at 60 °C in a sealed tube was found to be first order 4 half-lives with a rate constant of 3.78×10^{-4} M^{-1} s^{-1} ($t_{1/2}$ = 34 min). However, Cp^*WMe_3(NMe) did not form in a first-order manner, and the initial rate of appearance of Cp^*WMe_3(NMe) was approximately 40% of the rate of disappearance of **5b**. The first-order disappearance of **5b** could be explained by a rate-lim-

(43) Bullock, R. M. *J. Chem. Soc., Chem. Commun.* **1989**, 165.
(44) Chang, C. H.; Porter, R. F.; Brauer, S. H. *J. Am. Chem. Soc.* **1970**, *92*, 5313.
(45) Dickson, R. S.; Ibers, J. A. *J. Am. Chem. Soc.* **1972**, *94*, 2988.
(46) Ittel, S. D.; Ibers, J. A. *J. Organomet. Chem.* **1973**, *1973*, 389.
(47) Fochi, G.; Floriani, C.; Bart, J.; Giunchi, G. *J. Chem. Soc., Dalton Trans.* **1983**, 1515.
(48) Evans, W. J.; Drummond, D. K.; Chamberlain, L. R.; Doedens, R. J.; Bott, S. G.; Zhang, H.; Atwood, J. L. *J. Am. Chem. Soc.* **1988**, *110*, 4983.
(49) Durfee, L. D.; Hill, J. E.; Fanwick, P. E.; Rothwell, I. P. *Organometallics* **1990**, *9*, 75.

iting step change in the mode of bonding of the diazene ligand to the metal from η^2 to η^1, followed by rapid subsequent steps of unknown molecularity. The fact that $Cp^*WMe_3(NMe)$ is formed in a slower non-first-order reaction suggests that some intermediate should be observable, but neither a diamagnetic nor any paramagnetic species (by EPR) could be observed. A peculiar feature of this clean and high-yield reaction is that we have not yet been able to account for the 0.5 equiv of dimethyldiazene (nominally) that should be formed. Resonances consistent with a known product of rearrangement of *cis*-dimethyldiazene, $CH_2{=}NNH(CH_3)$,[50,51] could be observed by proton NMR, but only traces were present (ca. 10% of theory). Unlike the chemistry of the analogous diphenyldiazene complex (discussed below), addition of sodium amalgam does not increase the rate of formation of $Cp^*WMe_3(NMe)$ from **5b**. Further studies clearly will be required before details of this decomposition reaction can be proposed.

Methylation of **4b** with methyl triflate yields $[Cp^*WMe_3(\eta^2\text{-}NMeNMe_2)]^+$. A partial ($Cp^*$ disordered) X-ray structure of $[Cp^*WMe_3(\eta^2\text{-}NMeNMe_2)]^+$ showed that it has a structure analogous to that of $[Cp^*WMe_3(\eta^2\text{-}NHNH_2)]^+$. Therefore, the bonding mode observed in $Cp^*WMe_3(\eta^2\text{-}MeNNMe)$ cannot be ascribed to steric factors alone; the methyl group on the sp^2 nitrogen atom of the dimethyldiazene ligand *can* point toward the Cp^* ligand, i.e., formation of a W–nitrogen π bond could involve the $\pi_\parallel$ orbital instead of the observed $\pi_\perp$ orbital.

We hoped that reduction of $[Cp^*WMe_3(\eta^2\text{-}NMeNMe_2)]^+$ with Na/Hg in THF at −40 °C would allow us to observe $Cp^*WMe_3(NMeNMe_2)$, since this product cannot disproportionate via proton atom transfer. However, the product of the reaction is $Cp^*WMe_3(NMe)$ in 90% isolated yield (eq 6). We

$$[Cp^*WMe_3(\eta^2\text{-}NMeNMe_2)][OTf] \xrightarrow[THF,\,-40\ ^\circ C]{Na/Hg} Cp^*WMe_3(NMe) + Me_2NH \qquad (6)$$

speculate that since $Cp^*WMe_3(NMeNMe_2)$ cannot abstract $H^\bullet$ from another $Cp^*WMe_3(NMeNMe_2)$ (or H^+ from $[Cp^*WMe_3(NMeNMe_2)]^+$), it abstracts $H^\bullet$ from the solvent (THF) to form $Cp^*WMe_3(NMeHNMe_2)$, which then undergoes N–N bond cleavage to produce $Cp^*WMe_3(NMe)$ and dimethylamine.

Reduction of **1b** by sodium amalgam or sodium naphthalenide also yields $Cp^*WMe_3(NMe)$ (eq 7, Table III) plus a significant

$$\underset{\mathbf{1b}}{[Cp^*WMe_3(\eta^2\text{-}NHMeNHMe)]OTf} \xrightarrow[-\,NH_2Me]{Na/Hg} Cp^*WMe_3(NMe) \qquad (7)$$

amount of $[Cp^*WMe_3(\eta^2\text{-}NMeNHMe)][OTf]$. Formation of $Cp^*WMe_3(NMe)$ can be understood if $Cp^*WMe_3(\eta^2\text{-}NHMeNHMe)$ (**3b**) is formed and undergoes N–N bond cleavage, possibly in an acid-catalyzed reaction. However, it is not clear how $[Cp^*WMe_3(\eta^2\text{-}NMeNHMe)][OTf]$ is formed. Formation of $[Cp^*WMe_3(\eta^2\text{-}NMeNHMe)]$ nominally requires loss of a hydrogen atom from **1b**. We will see other examples of reactions later in which dihydrogen actually is observed. Formation of $[Cp^*WMe_3(\eta^2\text{-}NMeNHMe)][OTf]$ from **1b** is one of the several reactions involving substituted hydrazine or hydrazido complexes that are not observed for the parent hydrazine or hydrazido complexes and serves as a warning that it can be dangerous to extrapolate results observed in substituted hydrazine or hydrazido systems to the parent system.

Reactions Involving 1,2-Diphenylhydrazine. Addition of 1,2-diphenylhydrazine to $Cp^*WMe_3(OTf)$ in ether did not yield $[Cp^*WMe_3(\eta^2\text{-}NHPhNHPh)][OTf]$ (**1c**). Instead, a slow reaction produced a light yellow solid over a period of 24 h that was shown to consist of a mixture of anilinium triflate and $[Cp^*WMe_3(\eta^2\text{-}NPhNHPh)][OTf]$ (**4c**) in >45% yield (>90% of theory); $Cp^*WMe_3(NPh)$[36] could be recovered in yields of 36–42% (ca. 80% of theory) from the ethereal supernate. We propose that **1c** forms but that it decomposes via reactions (eqs 8–11) that are

$$Cp^*WMe_3(OTf) + PhNHNHPh \longrightarrow [Cp^*WMe_3(\eta^2\text{-}PhNHNHPh)][OTf]\ (\mathbf{1c})$$
$$\xrightarrow{-\,H^+} Cp^*WMe_3(\eta^2\text{-}PhNNHPh)\ (\mathbf{2c}) \qquad (8)$$

$$2\mathbf{c} \longrightarrow 0.5\ Cp^*WMe_3(\eta^2\text{-}PhNNPh)\ (\mathbf{5c}) + 0.5\ Cp^*WMe_3(\eta^2\text{-}PhHNNHPh)\ (\mathbf{3c}) \qquad (9)$$

$$3\mathbf{c} \xrightarrow{+\,0.5\ H^+} 0.5\ Cp^*WMe_3(NPh) + 0.5\ PhNH_3^+ \qquad (10)$$

$$5\mathbf{c} \xrightarrow{+\,0.5\ H^+} 0.5\ [Cp^*WMe_3(NPhNHPh)]^+\ (\mathbf{4c}) \qquad (11)$$

analogous to those we have proposed earlier in this paper. The two methyl ligands cis to the hydrazido ligand in **4c** are inequivalent in the proton NMR spectrum, consistent with the hydrazido ligand being bound in an η^2 fashion. We presume that the molecular structure of **4c** is analogous to that of **4a** and that the molecular structure of **1c** is analogous to that of **1a**.

Triethylamine is not a strong enough base to deprotonate $[Cp^*WMe_3(\eta^2\text{-}NPhNHPh)]^+$ (**4c**), a result that is analogous to that observed for **4b**. However, sodium hydride in THF will deprotonate **4c** to give $Cp^*WMe_3(\eta^2\text{-}PhNNPh)$ (**5c**) in 94% yield as dark red crystals (eq 12). We presume that the structure of

$$\underset{\mathbf{4c}}{[Cp^*WMe_3(\eta^2\text{-}PhNNHPh)][OTf]} \xrightarrow[-H_2,\,-NaOTf]{NaH} \underset{\mathbf{5c}}{Cp^*WMe_3(\eta^2\text{-}PhNNPh)} \qquad (12)$$

5c is analogous to that of **5b**. The 300-MHz proton NMR spectrum of **5c** in $CDCl_3$ at 25 °C shows a sharp singlet for the methyl group trans to the diazene ligand and a broad average resonance for the two methyl ligands cis to the diazene ligand at 0.4 ppm. The equilibration process can be slowed on the NMR time scale at −40 °C; the proton chemical shifts for the two cis methyl ligands in the slow exchange limit are 0.69 and −0.04 ppm, and the two methyl resonances coalesce at ca. 10 °C. This behavior is analogous to that of $Cp^*WMe_3(\eta^2\text{-}MeNNMe)$ that we discussed earlier. Protonation of **5c** with triflic acid in ether yields an immediate precipitate of **4c** in 78% isolated yield. Lutidinium triflate also protonates **5c**, but the reaction requires about 15 min to go to completion.

Reduction of **4c** by either Na/Hg or cobaltocene is believed to yield $Cp^*WMe_3(NPhNHPh)$, which disproportionates to **5c** and $Cp^*WMe_3(NHPhNHPh)$, which subsequently decomposes to $Cp^*WMe_3(NPh)$ and $PhNH_2$ (Scheme II; eq 13). The high

$$\underset{\mathbf{4c}}{[Cp^*WMe_3(\eta^2\text{-}PhNNHPh)][OTf]} \xrightarrow[-NaOTf\ -\ PhNH_2]{Na/Hg,\ THF} Cp^*Me_3W(NPh) + \mathbf{5c} \qquad (13)$$

solubilities of both $Cp^*WMe_3(NPh)$ and **5c** in pentane made their separation difficult, so their yields could be determined only by NMR methods. The ratio between them varied, but the amount of $Cp^*WMe_3(NPh)$ was never less than the amount of **5c**. When the reaction was run in C_6D_6 the ratio of the two was 1:1 after 2 h, but after 5 h the ratio of $Cp^*WMe_3(NPh)$ to **5c** was 1.3:1. In contrast to **5b**, **5c** was stable at 65 °C in C_6D_6 for 4 days. However, again in contrast to **5b**, **5c** is reduced by sodium amalgam in C_6D_6; in 16 h, $Cp^*WMe_3(NPh)$ is obtained in ca. 65% yield. Facile reduction of **5c** to $Cp^*WMe_3(NPh)$ is the likely reason why reduction of **4c** yields more $Cp^*WMe_3(NPh)$ than **5c**, especially at long reaction times.

Reactions Involving Methylhydrazine and 1,1-Dimethylhydrazine. Addition of methylhydrazine to $Cp^*WMe_3(OTf)$ yields $[Cp^*WMe_3(\eta^2\text{-}NH_2NHMe)][OTf]$ (**1d**) quantitatively. Deprotonation of **1d** (Table II) leads to relatively complex chemistry because either $Cp^*WMe_3(NHNHMe)$ (**2d**) or $Cp^*WMe_3(NMeNH_2)$ (**2d′**) can form and both pathways of decomposition shown in Schemes I and II are possible for **2d**. Deprotonation of **1d** with DBU in THF yields an equimolar mixture of $Cp^*WMe_3(\eta^1\text{-}NNHMe)$, $Cp^*WMe_3(NH)$, and methylamine, analogous to the results observed for **1a**. When **1d** is treated with NEt_3 in THF a 1:2 mixture of $Cp^*WMe_3(NH)$ and $Cp^*WMe_3(\eta^1\text{-}NNHMe)$ is observed. Curiously, deprotonation of **1d** with NEt_3 in dichloromethane cleanly generates $Cp^*WMe_3(\eta^1\text{-}NNHMe)$ in 77% yield (Table II), and dihydrogen

(50) Ackermann, M. N.; Craig, N. C.; Isberg, R. R.; Lauter, D. M.; MacPhail, R. A.; Young, W. G. *J. Am. Chem. Soc.* **1977**, *99*, 1661.
(51) Hutton, R. F.; Steel, C. *J. Am. Chem. Soc.* **1964**, *86*, 745.

was observed by ^1H NMR in a sealed tube. Both the high yield of $Cp^*WMe_3(\eta^1\text{-}NNHMe)$ and the observation of dihydrogen can be explained by a type of reaction (eq 14) that has not been

$$Cp^*WMe_3(NHNHMe) \longrightarrow 0.5\ H_2 + Cp^*WMe_3(\eta^1\text{-}NNHMe) \quad (14)$$

observed before in the Cp^*WMe_3 system in the absence of a good reducing agent such as sodium amalgam. This type of reaction could account for the excess $Cp^*WMe_3(\eta^1\text{-}NNHMe)$ observed when **1d** is treated with NEt_3 in THF and illustrates again some of the differences between substituted and unsubstituted hydrazine or hydrazido complexes. The details of the reaction shown in eq 14 are obscure at this stage. However, again we observe that when **1d** is deprotonated by DBU (presumably rapidly and essentially irreversibly), $Cp^*WMe_3(\eta^1\text{-}NNHMe)$, $Cp^*WMe_3(NH)$, and methylamine are formed in high yield with few side reactions. Either $Cp^*WMe_3(NHNHMe)$ (**2d**) or $Cp^*WMe_3(NMeNH_2)$ (**2d'**) could disproportionate to yield $Cp^*WMe_3(\eta^1\text{-}NNHMe)$, $Cp^*WMe_3(NH)$, and methylamine. The most straightforward reaction would appear to be disproportionation of **2d** to give $Cp^*WMe_3(\eta^1\text{-}NNHMe)$ and $Cp^*WMe_3(NH_2NHMe)$, followed by decomposition of the latter to $Cp^*WMe_3(NH)$ and methylamine.

Reduction of **1d** in THF yields a mixture of $Cp^*WMe_3(NH)$, $Cp^*WMe_3(NMe)$, and $Cp^*WMe_3(\eta^1\text{-}NNHMe)$ (Table III). We speculate that $Cp^*WMe_3(NH_2NHMe)$ (**3d**) is an intermediate in this reaction and that the N–N bond is cleaved to yield either $Cp^*WMe_3(NH)$ and methylamine or $Cp^*WMe_3(NMe)$ and ammonia (eq 15). $Cp^*WMe_3(\eta^1\text{-}NNHMe)$, which often comprises ca. 50% of the reaction product, is nominally the product of loss of dihydrogen from **3d**. The manner in which it is formed is perhaps related to the manner in which it forms upon deprotonation of **1d**. It should be noted that formation of $Cp^*WMe_3(\eta^1\text{-}NNHMe)$ does not depend dramatically on the type of reductant or the solvent. It is puzzling, however, that if $Cp^*WMe_3(NH_2NHMe)$ is involved in both the deprotonation (disproportionation) and reduction of **1d**, $Cp^*WMe_3(NMe)$ is formed only in the reduction reaction. Perhaps $Cp^*WMe_3(NH_2NHMe)$ can react directly with sodium amalgam to yield $Cp^*WMe_3(NMe)$.

$$[Cp^*WMe_3(\eta^2\text{-}NH_2NHMe)]OTf \ (\mathbf{1d}) \xrightarrow[-NH_2Me,\ -NH_3]{Na/Hg} \text{"}Cp^*WMe_3(NH_2NHMe)\text{"} \ (\mathbf{3d})$$

$$\longrightarrow Cp^*WMe_3(NH) + Cp^*WMe_3(NMe) \quad (15)$$

Addition of NH_2NMe_2 to $Cp^*WMe_3(OTf)$ in ether at −40 °C yields $[Cp^*WMe_3(NH_2NMe_2)][OTf]$ (**1e**) as a light orange solid. Unfortunately, **1e** cannot be isolated in analytically pure form because $[NH_3NMe_2][OTf]$ cannot be removed entirely in recrystallizations. Deprotonation of **1e** with either NEt_3 or DBU in THF or dichloromethane yields a mixture of $Cp^*WMe_3(NH)$, dimethylamine, and $Cp^*WMe_3(\eta^1\text{-}NNMe_2)$ that we propose arise via disproportionation of intermediate $Cp^*WMe_3(NHNMe_2)$ (**2e**) (eq 16, Table II). Dimethylamine was observed by ^1H NMR in these reactions in an amount that equaled the amount of $Cp^*WMe_3(NH)$.

$$[Cp^*WMe_3(\eta^2\text{-}NH_2NMe_2)][OTf] \ (\mathbf{1e}) \xrightarrow{DBU} Cp^*WMe_3(NHNMe_2) \ (\mathbf{2e}) \longrightarrow$$

$$0.5\ Cp^*WMe_3(NH) + 0.5\ Cp^*WMe_3(\eta^1\text{-}NNMe_2) + 0.5\ NHMe_2 \quad (16)$$

Reduction of **1e** with sodium amalgam in ether or sodium naphthalenide in THF yields $Cp^*WMe_3(NH)$ and $NHMe_2$ (Table III), the expected products of N–N bond cleavage in $Cp^*WMe_3(\eta^2\text{-}NH_2NMe_2)$ (**3e**). However, some $Cp^*WMe_3(\eta^1\text{-}NNMe_2)$ (eq 17) is also formed by a reaction that nominally consists of loss of dihydrogen from **3e**. This reaction should be compared to that which yields $Cp^*WMe_3(\eta^1\text{-}NNHMe)$ upon reduction of $[Cp^*WMe_3(\eta^2\text{-}NH_2NHMe)]^+$ (see above). As in other reactions of this type, details of formation of $Cp^*WMe_3(\eta^1\text{-}NNMe_2)$ from **3e** are unclear at this stage.

$$[Cp^*WMe_3(\eta^2\text{-}NH_2NMe_2)][OTf] \ (\mathbf{1e}) \xrightarrow[\text{ether, -40 °C}]{Na/Hg} \underset{\text{(major)}}{Cp^*WMe_3(NH)} + \underset{\text{(minor)}}{Cp^*WMe_3(\eta^1\text{-}NNMe_2)} \quad (17)$$

Table VI. Stoichiometric Formation of Ammonia from $WCp^*Me_3(\eta^1\text{-}NNH_2)$ or $[WCp^*Me_3(\eta^2\text{-}NH_2NH_2)]^+$ [a]

complex	reducing agent	proton source	yield[c]
$WCp^*Me_3(\eta^1\text{-}NNH_2)$	Zn/Hg	Lut·HCl	92(2)[d]
	Zn/Hg	phenol	65(1)
	Zn/Hg	TIPT[b]	71(2)
	Zn/Hg	H_2	60(2)[e]
$[WCp^*Me_3(\eta^2\text{-}NH_2NH_2)]^+$	Cp_2Co	Lut·HCl	92(2)
	Zn/Hg	Lut·HCl	91(1)
	$SnCl_2$	Lut·HCl	45(1)[e]
	Zn/Hg	phenol	88(2)
	Zn/Hg	H_2	57(3)[e]

[a] See Experimental Section for conditions. [b] TIPT = 2,3,5-triisopropylbenzenethiol. [c] Unless otherwise noted, each reaction was done three times; the range (±) is quoted in parentheses. [d] Reaction done six times. [e] Reaction done twice.

Table VII. Effect of Proton Source on Ammonia Formation from $WCp^*Me_3(\eta^1\text{-}NNH_2)$ [a]

proton source	pK_a	yield[b]
Py·HCl	5.2	29(2)
Py·HOTf	5.2	72(2)
Py·HBF_4	5.2	52(2)
Py·HBR_4	5.2	75(4)[d]
Lut·HCl	5.7	92(2)[c]
Lut·HOTf	5.7	87(1)
Lut·HBF_4	5.7	56(2)
Lut·HBR_4	5.7	70(2)[d]
Imid·HCl	7.0	71(2)
Imid·HOTf	7.0	75(1)[d]
Imid·HBF_4	7.0	68(1)[d]
NBu_3·HCl	10.0	81(1)[d]
NBu_3·HOTf	10.0	71(1)
NBu_3·HBF_4	10.0	45(3)

[a] See Experimental Section for conditions. R = 3,5-$C_6H_3(CF_3)_2$; Imid = imidazole. [b] Unless otherwise noted, each reaction was done three times; the range (±) is shown in parentheses. [c] Reaction was done six times. [d] Reaction was done twice.

Generation of Ammonia. Ammonia can be generated from low-oxidation-state metal dinitrogen complexes by adding only protons; the transition metal serves as the source of electrons.[1,2] However, analogous reactions at high-oxidation-state metal centers require an external source of several electrons in order to obtain yields of ammonia close to theory. A potential problem in this circumstance is the concurrent reduction of protons to dihydrogen. In an earlier publication we presented preliminary results for the formation of ammonia from several hydrazido(4−) and hydrazido(2−) complexes containing the Cp^*WMe_3 core using zinc amalgam and 2,6-lutidinium chloride as the reductant and proton source, respectively.[35] A more thorough study is presented here.

The ammonia yields obtained upon reducing $Cp^*WMe_3(\eta^1\text{-}NNH_2)$ or $[Cp^*WMe_3(\eta^2\text{-}NH_2NH_2)]^+$ under various conditions are shown in Tables VI and VII. The largest yield of ammonia was observed when lutidinium chloride was the proton source and either zinc amalgam or cobaltocene was employed as the reducing agent (Table VI). Although the yield of ammonia varied with the pK_a of the acid employed (Table VII), it did not vary in a clear and systematic fashion. Overall, these results suggest that the relative acidity of the proton in the range we investigated is not an overwhelmingly important factor in the formation of ammonia from these high-oxidation-state complexes. We do not want to overinterpret these findings since the results of many of these reactions may differ for a combination of reasons, such as the low solubility of some proton sources in THF and the heterogeneous nature of most of the reactions.

One possible complication in systems involving the Cp^*WMe_3 core is protonation of one or more methyl groups on the metal, since the N–N bond may not be cleaved as efficiently in Cp^*WMe_2X derivatives as in Cp^*WMe_3 derivatives. $Cp^*WMe_3(\eta^1\text{-}NNH_2)$ reacts with HX (X = Cl, OTf, BF_4, B-[3,5-$C_6H_3(CF_3)_2]_4$) to produce $[Cp^*WMe_3(\eta^2\text{-}NHNH_2)][X]$ complexes.[42] However, $[Cp^*WMe_3(\eta^2\text{-}NHNH_2)][Cl]$ is unstable

Table VIII. Catalytic Reduction of Hydrazine to Ammonia[a]

complex	N_2H_4 (equiv)	NH_3 (equiv)	total conversion[c] (%)
$WCp^*Me_3(\eta^1\text{-}NNH_2)$	0	1.80	92(1)[d]
	3	6.72	84(2)
	6	10.92	78(2)[e]
$[WCp^*Me_3(\eta^2\text{-}NH_2NH_2)]^+$	0	1.88	93(1)[d]
	0[b]	1.76	87(2)
	2	5.88	98(2)
	2[b]	4.58	85(2)[e]
	3	7.28	92(2)
	3[b]	6.64	82(2)
	4	8.48	85(2)[e]
	6	11.32	83(1)
	8	14.94	81(2)
	10	15.84	72(2)[e]

[a] See Experimental Section for details. [b] Phenol is used as proton source. [c] Unless otherwise noted, each reaction was done three times; the range (±) is shown in parentheses. [d] Reaction was done six times. [e] Reaction was done twice.

toward loss of methane to give *trans*-$Cp^*WMe_2Cl(\eta^1\text{-}NNH_2)$. Methane loss is slow when X = OTf and is not observed when X = BF_4 or $B(Ph_f)_4$. Therefore, we were surprised to find that the best ammonia yields were obtained consistently when X = Cl or OTf, not when X is relatively noncoordinating, and that when $Cp^*WMe_2Cl(\eta^1\text{-}NNH_2)$[42] was reduced under the same conditions as $Cp^*WMe_3(\eta^1\text{-}NNH_2)$ an 85% yield of ammonia was obtained, virtually as high (93–94%) as that obtained upon reducing $Cp^*WMe_3(\eta^1\text{-}NNH_2)$. Therefore, it does not appear that the Cp^*WMe_3 core per se has special properties that make ammonia formation favorable; it is perhaps a more general feature of the Cp^*WMe_3 complex that leads to facile N–N bond cleavage.

Catalytic Reduction of Hydrazine. Hydrazine can be reduced catalytically using either $Cp^*WMe_3(\eta^1\text{-}NNH_2)$ or $[Cp^*WMe_3(\eta^2\text{-}NH_2NH_2)]^+$ to give ammonia in yields that exceed the yields expected (66.7%) if hydrazine simply disproportionates to dinitrogen and ammonia (Table VIII). (Reduction studies were done in THF at room temperature over a period of 16–28 h employing zinc amalgam as the reducing agent and lutidinium chloride or phenol as the proton source.) The highest ammonia yields were observed when only a few equivalents of hydrazine were reduced. The decrease in the yield of ammonia when reduction of greater than 6 equiv of hydrazine is attempted suggests that side reactions severely limit catalyst longevity. Lower yields of ammonia were observed when phenol was employed as the proton source. The *idealized* catalytic cycle shown in Scheme III is based on the observed behavior of several hydrazido complexes of the type we have discussed here in addition to the known reaction between $Cp^*WMe_3(NH_2)$ and hydrazine to give 1 equiv of ammonia and $Cp^*WMe_3(NHNH_2)$. $Cp^*WMe_3(NHNH_2)$ is known to disproportionate to 0.5 equiv of $Cp^*WMe_3(NH)$, 0.5 equiv of ammonia, and 0.5 equiv of $Cp^*WMe_3(\eta^1\text{-}NNH_2)$, as we have discussed earlier in this paper. Disproportionation or protonation of $Cp^*WMe_3(NHNH_2)$ also could be an intimate feature of the catalytic reduction of hydrazine observed here, although in Scheme III we propose that $Cp^*WMe_3(NHNH_2)$ instead is protonated rapidly to give $[Cp^*WMe_3(\eta^2\text{-}NH_2NH_2)]^+$. The side reactions that limit catalyst longevity are not known.

Discussion

The only examples of structurally characterized bidentate, unsubstituted hydrazine complexes are $[Cp^*WMe_3(\eta^2\text{-}NH_2NH_2)][OTf]$ (**1a**), $[W(NAr)[2,6\text{-}NC_5H_3(CH_2Ntosyl)_2]\text{-}(Cl)(\eta^2\text{-}NH_2NH_2)]^+$,[52] $[(MeC(CH_2PPh_2)_3]Co(\eta^2\text{-}NH_2NH_2)]^{2+}$,[53] and $[Cp^*_2Sm(THF)(\eta^2\text{-}NH_2NH_2)]^+$.[54] Complexes containing substituted η^2 hydrazine ligands are also relatively rare.[55] The majority of structurally characterized transition-metal complexes that contain an unsubstituted hydrazine ligand are bimetallic. Examples include $[M(CO)_5]_2(\mu\text{-}NH_2NH_2)$ M = Cr, Mo, W), $[CpM(CO)_2]_2(\mu\text{-}NH_2NH_2)$ (M = Mn, Re) and related heterobimetallic complexes,[56] [Ru(biphenylenediporphyrinato)]$_2(\mu\text{-}NH_2NH_2)$,[57] $[NEt_4]_4\{[MoFe_3S_4Cl_2(O_2C_6Cl_4)]_2(\mu\text{-}S)(\mu\text{-}NH_2NH_2)\}$,[58] and $[M(O)(S_2)_2]_2(\mu\text{-}NH_2NH_2)$ (M = Mo or W).[59]

Reactions involving hydrazine or substituted hydrazines and transition-metal complexes are often complex. For example, the first dinitrogen complex, $[Ru(NH_3)_5(N_2)]^{2+}$, was originally prepared from "$RuCl_3(H_2O)_3$" and hydrazine hydrate.[60] (Hydrazine is both reduced to ammonia and oxidized to dinitrogen in this reaction.) Hydrazine is the source of ammonia in the ammonia adducts $M(CO)_5(NH_3)$, $CpM(CO)_2(NH_3)$,[56] and [Ru(biphenylenediporphyrinato)]$_2(NH_3)_2$,[56,57] and hydrazine is known also to yield nitrido complexes such as $M(N)X_2(PR_3)_n$ (n = 2 or 3; M = Re,[61–63] Tc;[64] X = halide), $Tc(N)(S_2CNEt_2)_2$,[65] and $K[ReN(H_2O)(CN)_4]$.[66] There also are examples of symmetric 1,2-disubstituted hydrazines NHRNHR (R = Me, Ph, etc.) being cleaved to form imido complexes such as $Re(NMe)Cl_3(PPh_3)$[67] or $[TaCl_2(NH_2Ph)]_2(\mu\text{-}Cl)_2(\mu\text{-}NPh)$[68] or amido complexes such as $Cp^*_2Sm(NHPh)(THF)$.[69] Therefore, facile cleavage of the N–N bond in hydrazine and substituted hydrazines and complex subsequent reactions are relatively common.

In view of the scarcity of hydrazine complexes, the complexity of reactions involving hydrazines, the possibility of reducing tungsten, and the possibility of losing protons from hydrazine to methyl groups on tungsten, it is surprising that **1a** and related

Scheme III

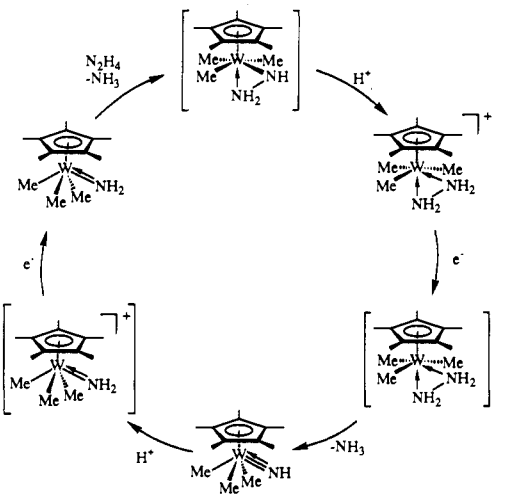

(52) Cai, S.; Schrock, R. R. *Inorg. Chem.* **1991**, *30*, 4105.
(53) Vogel, S.; Berth, A.; Huttner, G.; Klein, T.; Zsolnai, L.; Kremer, R. *Angew. Chem., Int. Ed. Engl.* **1991**, *30*, 303.
(54) Evans, W. J.; Kociok-Köhn, G.; Ziller, J. W. *Angew. Chem., Int. Ed. Engl.* **1992**, *31*, 1081.
(55) Bultitude, J.; Larkworthy, L. F.; Povey, D. C.; Smith, G. W.; Dilworth, J. R.; Leigh, G. J. *J. Chem. Soc., Chem. Commun.* **1986**, 1748.
(56) Sellmann, D. In *Recent Developments in Nitrogen Fixation*; Newton, W., Postgate, J. R., Rodriguez-Barrueco, C., Eds.; Academic Press: London, 1977; p 53.
(57) Collman, J. P.; Hutchinson, J. E.; Lopez, M. A.; Guilard, R.; Reed, R. A. *J. Am. Chem. Soc.* **1991**, *113*, 2794.
(58) Challen, P. R.; Koo, S.-M.; Kim, C. G.; Dunham, W. R.; Coucouvanis, D. *J. Am. Chem. Soc.* **1990**, *112*, 8606.
(59) Zhu, N.; Du, S.; Wu, X.; Lu, J. *Angew. Chem., Int. Ed. Engl.* **1992**, *31*, 87.
(60) Allen, A. D.; Senoff, C. V. *J. Chem. Soc., Chem. Commun.* **1965**, 621.
(61) Chatt, J.; Falk, C. D.; Leigh, G. J.; Paske, R. J. *J. Chem. Soc. (A)* **1969**, 2288.
(62) Chatt, J.; Garforth, J. D.; Johnson, N. P.; Rowe, G. A. *J. Chem. Soc.* **1964**, 1012.
(63) Jabs, W.; Herzog, S. *Z. Chem.* **1972**, *12*, 268.
(64) Kaden, L.; Lorenz, B.; Schmidt, K.; Sprinz, H.; Wahren, M. *Isotopenpraxis* **1981**, *17*, 174.
(65) Baldas, J.; Bonnyman, J.; Pojer, P. M.; Williams, G. A.; Mackay, M. F. *J. Chem. Soc., Dalton Trans.* **1981**, 1798.
(66) Lock, C. J. L.; Wilkinson, G. *J. Chem. Soc.* **1964**, 2281.
(67) Chatt, J.; Dilworth, J. R.; Leigh, G. J. *J. Chem. Soc. (A)* **1970**, 2239.
(68) Canich, J. M.; Cotton, F. A.; Falvello, L. R.; Duraj, S. A. *Inorg. Chim. Acta* **1988**, *143*, 185.
(69) Evans, W. J.; Kociok-Köhn, G.; Leong, V. S.; Ziller, J. W. *Inorg. Chem.* **1992**, *31*, 3592.

hydrazine complexes of type **1** are stable. The stability of **1a** toward bimolecular reactions might be ascribed to the fact that **1a** is a pseudooctahedral 17-electron species that contains no basic sites (at least until N_β in the η^2-NH_2NH_2 ligand dissociates to yield an η^1-NH_2NH_2 ligand). Activation of a proton in the η^2-NH_2NH_2 ligand through an initial "agostic" interaction of the electron density in an N–H bond with an empty orbital on the metal is not possible in **1a**, since the only available orbital on the metal contains one electron. The stability of **1a** is especially striking in contrast to the instability of "Cp*$WMe_3(NH_2NH_2)$", a d^2 complex.

The ready disproportionation of Cp*$WMe_3(NHNH_2)$ and substituted analogs is a recurring theme in this work, as well as for hydrazido complexes of other transition metals and even lanthanides.[69] In a related tungsten system it was found that addition of hydrazine to $W(NPh)Me_4$ yielded methane and structurally characterized $[W(NPh)Me_3]_2(\mu$-η^1,η^1-$NH_2NH_2)(\mu$-η^2,η^2-NHNH) (eq 18).[70] One can imagine that this product arises

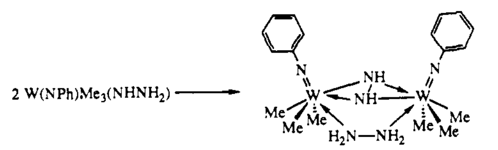

(18)

via a bimolecular reaction involving initially formed $W(NPh)Me_3(NHNH_2)$. It should be noted that $W(NPh)Me_3(NHNH_2)$ is a d^0 species while Cp*$WMe_3(NHNH_2)$ is a d^1 species, so no electrons are available for N–N bond cleavage in $W(NPh)Me_3(NHNH_2)$ and the diazene or "1,2-hydrazido(2−)" ligand that results from proton transfer (eq 19) simply binds side-on in order

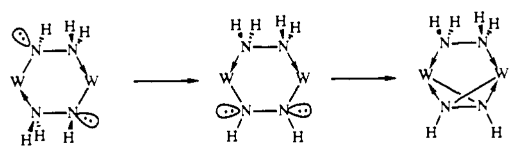

(19)

to achieve an 18-electron count at each metal. On the basis of these results, one might propose a similar bimolecular reaction of Cp*$WMe_3(\eta^1$-$NHNH_2)$ with itself to give an intermediate that contains both hydrazine and diazene, as shown in eq 20. Dissociation of this intermediate into Cp*$WMe_3(NH_2NH_2)$ and Cp*WMe_3(NHNH) would then lead to Cp*WMe_3(NH) plus ammonia (from Cp*$WMe_3(NH_2NH_2)$) and Cp*$WMe_3(\eta^1$-$NNH_2)$ (upon rearrangement of the diazene ligand in Cp*WMe_3(NHNH)). However, a more consistent explanation, in our opinion, in part since Cp*$WMe_3(\eta^2$-$NNH_2)$ was observed at low temperature, is that H_α is removed in an η^2-$NHNH_2$ species, perhaps in an intermediate involving more than one hydrogen bond (eq 21). Another argument in favor of an intermediate such as

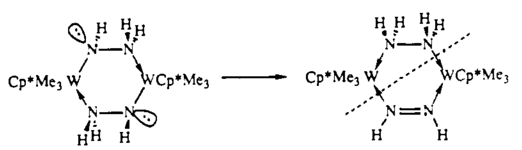

(20)

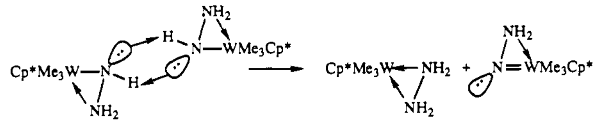

(21)

that shown in eq 21 is that even though relatively crowded bimolecular complexes involving the Cp*WMe_3 core can form (e.g., $\{[$Cp*$WMe_3]_2(\mu$-N)$\}^{+}$[71]), intermediates such as those shown in eqs 19 and 20 would seem to be sterically less accessible than that shown in eq 21.

The 18-electron tungsten(IV) hydrazine adduct Cp*$WMe_3(\eta^2$-$NH_2NH_2)$ (**3a**) and related substituted derivatives appear to play central roles in much of the chemistry described here. Everything we have observed so far is consistent with N–N bond cleavage in species of this sort in the *absence* of protons. (N–N bond cleavage in the presence of protons can also be fast and may predominate; it is considered below.) If the η^2-NH_2NH_2 ligand remains bound to the metal, a proton must migrate from one nitrogen to the other. The only lone pair of electrons that could assist that migration is on the metal in either the $\pi_\parallel$ orbital or the $\pi_\perp$ orbital, depending on whether the hydrazine is bound parallel or perpendicular to the plane of the Cp* ligand. It is possible to imagine how a proton might be transferred if the two d electrons are in the $\pi_\perp$ orbital and the hydrazine lies approximately parallel to the plane of the Cp* ligand (eq 22). In this circumstance the lobe of the $\pi_\perp$ orbital roughly points toward the NH protons that point away from the Cp* ligand (bold in eq 22).

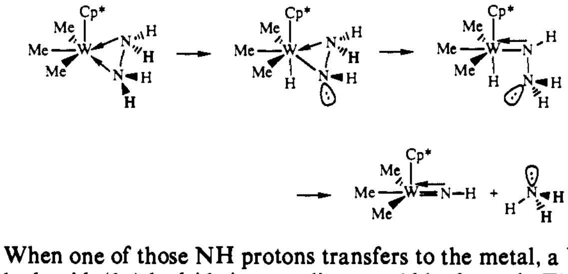

(22)

When one of those NH protons transfers to the metal, a W(VI) hydrazido(1−) hydride intermediate would be formed. This is an attractive intermediate since Cp*$WMe_4(\eta^2$-$NHNH_2)$ is a stable, structurally characterized, fluxional species in which the N–N bond lies approximately parallel to the plane of the Cp* ligand;[34] the only difference is that in the *solid* state the lone pair on the NH points *toward* the Cp* ligand in Cp*$WMe_4(\eta^2$-$NHNH_2)$, not away from the Cp* ligand.[34,42] If Cp*$WMe_3(H)(\eta^1$-$NHNH_2)$ forms from Cp*$WMe_3(H)(\eta^2$-$NHNH_2)$, a proton could then transfer to the lone pair on N_β to complete the formation of ammonia and Cp*WMe_3(NH) (eq 22). It should be noted that $[$Cp*$ReMe_3(\eta^2$-$NH_2NH_2)]^+$, the Re(V) d^2 rhenium analog of unobserved Cp*$WMe_3(\eta^2$-$NH_2NH_2)$, is a stable species.[72] $[$Cp*$ReMe_3(\eta^2$-$NH_2NH_2)]^+$ might not lose ammonia, because $[$Cp*$ReMe_3(NH)]^+$ would have to form, and all we have observed so far suggests that Re(VII) is a less accessible oxidation state than W(VI) in complexes of this type. A 1,2 proton shift from the coordinated N_α in Cp*$WMe_3(\eta^1$-$NH_2NH_2)$ to the adjacent lone pair on N_β would be a shorter route to Cp*WMe_3(NH) and ammonia, but the orbital that contains the lone pair on N_β in Cp*$WMe_3(\eta^1$-$NH_2NH_2)$ does not point toward the hydrogen atom on N_α, so direct 1,2 migration of H_α would not seem to be as favorable as formation of an intermediate W(VI) hydride complex. A potentially important feature of the mechanism shown in eq 22 is the ability of the metal to form a strong W–N π bond and thereby "prepare" the other end of the polarized hydrazido(1−) ligand to receive the proton from the metal.

Another mechanism that involves oxidation of W(IV) to W(VI) is shown in eq 23. Subsequent α-hydrogen abstraction would

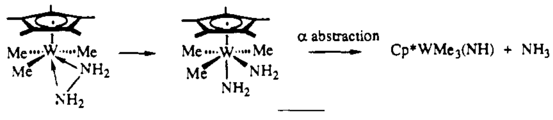

(23)

then yield ammonia and Cp*WMe_3(NH). Isoelectronic Cp*$W(CH_3)_5$ is known to decompose readily by α-hydrogen abstraction to yield unstable Cp*$WMe_3(CH_2)$ and CH_4,[73] so if Cp*$WMe_3(NH_2)_2$ were to form, one can accept the possibility that it would decompose selectively to Cp*WMe_3(NH) and NH_3; formation of a tungsten–nitrogen pseudotriple bond should be favored over formation of a tungsten–carbon double bond.

(70) Blum, L.; Williams, I. D.; Schrock, R. R. *J. Am. Chem. Soc.* **1984**, *106*, 8317.
(71) Glassman, T. E.; Liu, A. H.; Schrock, R. R. *Inorg. Chem.* **1991**, *30*, 4723.
(72) Vale, M. G.; Schrock, R. R. *Organometallics* **1991**, *10*, 1661.
(73) Liu, A. H.; Murray, R. C.; Dewan, J. C.; Santarsiero, B. D.; Schrock, R. R. *J. Am. Chem. Soc.* **1987**, *109*, 4282.

Cleavage of the N–N bond in the *presence* of protons could be quite different mechanistically than cleavage in the absence of protons. The two most likely sites for protonation are the metal in $Cp^*WMe_3(\eta^2\text{-}NH_2NH_2)$ or $Cp^*WMe_3(\eta^1\text{-}NH_2NH_2)$ or the lone pair on N_β in $Cp^*WMe_3(\eta^1\text{-}NH_2NH_2)$. Protonation at the metal in $Cp^*WMe_3(\eta^2\text{-}NH_2NH_2)$ would yield $[Cp^*WMe_3(H)(\eta^2\text{-}NH_2NH_2)]^+$ initially. However, only upon forming $[Cp^*WMe_3(H)(\eta^1\text{-}NH_2NH_2)]^+$, the species that also would be obtained upon protonating $Cp^*WMe_3(\eta^1\text{-}NH_2NH_2)$ at the metal, could the proton then transfer to the uncoordinated nitrogen atom to yield ammonia and $[Cp^*WMe_3(NH_2)]^+$. Addition of a proton to the electron pair on N_β in $Cp^*WMe_3(\eta^1\text{-}NH_2NH_2)$ could lead directly to ammonia and $[Cp^*WMe_3(NH_2)]^+$ (eq 24). Although

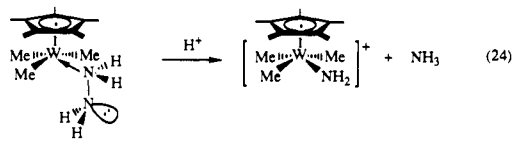

(24)

$Cp^*WMe_3(NH_2)$ is known, $[Cp^*WMe_3(NH_2)]^+$ is not, perhaps because an agostic interaction between an N–H bond and the d^0 metal causes $[Cp^*WMe_3(NH_2)]^+$ to lose a proton readily to give $Cp^*WMe_3(NH)$, a stable species.[36] Nevertheless, $[Cp^*WMe_3(NH_2)]^+$ could be involved in a sequence of protonation/reduction reactions that ultimately would yield the second equivalent of ammonia. We have no way of knowing at this stage whether a pathway for N–N bond cleavage that involves protons is competitive with that for intramolecular (proton-free) N–N bond cleavage under the conditions we have employed for generating ammonia.

Both the disproportionation reaction of $Cp^*WMe_3(NHNH_2)$ (**2a**) and the N–N bond cleavage reaction involving **3a** are competing with side reactions that are not well understood at this time. The most unusual are those involving substituted hydrazido or hydrazine ligands in which dihydrogen is formed. For example, deprotonation of $[Cp^*WMe_3(\eta^2\text{-}N_2H_3Me)]^+$ by triethylamine should yield $Cp^*WMe_3(NHNHMe)$ and $Cp^*WMe_3(NMeNH_2)$, followed by disproportionation of each to produce a mixture of $Cp^*WMe_3(NMe)$ and $Cp^*WMe_3(NH)$. Instead, $Cp^*WMe_3(\eta^1\text{-}NNHMe)$ is formed in almost 80% yield. If the same type of reaction were to take place upon deprotonation of $[Cp^*WMe_3(\eta^2\text{-}NH_2NH_2)]^+$ (**1a**), then only $Cp^*WMe_3(\eta^1\text{-}NNH_2)$ would be formed and no ammonia. That is not the case. Therefore, we are wary about drawing conclusions or generalizing about unsubstituted hydrazine and hydrazido complexes on the basis of results obtained for substituted hydrazine and hydrazido species. In future studies it may be more profitable to focus on unsubstituted hydrazine and hydrazido species.

There are a limited number of reports of homogeneous catalytic reduction of hydrazine to ammonia; in general, the actual catalytically active species are unknown and the mechanisms are ill-defined.[74-78] In the molybdenum nitrogenase system, hydrazine has been obtained upon quenching the active enzyme,[79,80] but its origin is uncertain. Hydrazine itself is a substrate for the nitrogenase enzyme under some conditions.[81-83] These findings

Scheme IV

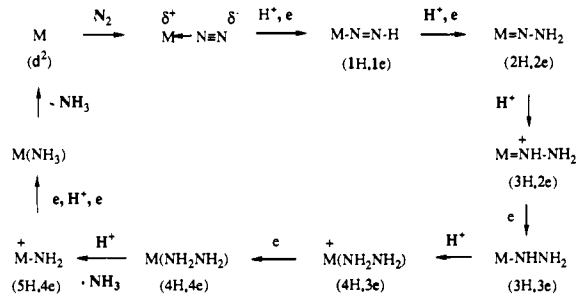

would be consistent with a proposed intermediate that contains bound hydrazine and with a proposal that ammonia is formed from that bound hydrazine.

There are several interesting features of the chemistry described here that differ significantly from hydrazido chemistry of metals in low oxidation states[1-3] and that together support a scheme for dinitrogen reduction (Scheme IV) that differs in several important details from previously proposed schemes. One feature is that starting at the $W{=}NNH_2$ stage, monoprotonation of a neutral species is always followed by reduction of a cationic species by one external electron. (Eight separate one-electron reductions are involved in reduction of dinitrogen and eight protons to ammonia and dihydrogen by molybdenum-containing nitrogenases.) Similar monoprotonation/reduction steps have been observed in low-oxidation-state Mo and W dinitrogen and hydrazido complexes, but although a large number of intermediate hydrazido and NH_x intermediates have been observed, it is rare to observe several types by monoprotonation/reduction steps in which the metal core is the same. A second potentially important feature of Cp^*WMe_3 hydrazine and hydrazido chemistry is the η^2-bonding of N_2H_x fragments using three frontier orbitals ($2\pi,1\sigma$) while maintaining the basic Cp^*WMe_3 core. While the chemistry that we have outlined does not prove that η^2-bonding of N_2H_x fragments is required for a controlled N–N bond cleavage, it strongly suggests that η^2-bonding involving three ($2\pi,1\sigma$) orbitals yields more stable intermediates in a sequence of steps leading to N–N bond cleavage. And finally, the most important feature of the Cp^*WMe_3 system in terms of N–N bond cleavage is that hydrazine (bound to the metal) is believed to lie *on* the pathway to ammonia (Scheme IV); it is not the product of a side reaction, a view that appears to prevail in the chemistry of lower-oxidation-state complexes.

We have shown here that the N–N bond in a high-oxidation-state tungsten N_2H_x complex can be split to give ammonia efficiently in the presence of protons and electrons. Since we have also shown that this same Cp^*WMe_3 core will activate dinitrogen to give a $[Cp^*WMe_3]_2(\mu\text{-}N_2)$ complex,[33] we believe that it should be possible to reduce dinitrogen to ammonia catalytically at a single high-oxidation-state (d^0, d^1, or d^2) Mo or W center in the presence of a proton source. We will be searching for a metal core that is stable to protons and electrons, preferably one that also prevents bimolecular reactions of intermediate N_2H_x complexes. An interesting and important question is whether protons will be reduced to dihydrogen at this same catalytic site and whether dihydrogen complexes are an important feature of the dinitrogen reduction process. If dihydrogen is made at the same site at which dinitrogen is reduced, then ultimately a way of limiting the rate of proton reduction at that site ("gating") must be devised in order to allow dinitrogen to compete successfully with protons at that site.

Experimental Section

General Procedures. Solvents were dried and degassed prior to use and distilled from molten sodium (toluene), sodium/benzophenone (ether, tetrahydrofuran, pentane), calcium hydride (dichloromethane), or P_2O_5 (acetonitrile). (Pentane was first washed with 5% HNO_3/H_2SO_4 and dried using tetraglyme to solvate the sodium.) All preparations were conducted under a nitrogen atmosphere in a Vacuum Atmospheres drybox, under argon when using Schlenk techniques, or on a high vacuum line ($<10^{-4}$ Torr).

(74) Hozumi, Y.; Imasaka, Y.; Tanaka, K.; Tanaka, T. *Chem. Lett.* **1983**, 897.
(75) Schrauzer, G. N.; Kiefer, G. W.; Tano, K.; Doemeny, P. A. *J. Am. Chem. Soc.* **1974**, *96*, 641.
(76) Schrauzer, G. N. *Angew. Chem., Int. Ed. Engl.* **1975**, *14*, 514.
(77) Schrauzer, G. N.; Robinson, P. R.; Moorehead, E. L.; Vickrey, T. M. *J. Am. Chem. Soc.* **1976**, *98*, 2815.
(78) Block, E.; Ofori-Okai, G.; Kang, H.; Zubieta, J. *J. Am. Chem. Soc.* **1992**, *114*, 758.
(79) Thorneley, R. N. F.; Eady, R. R.; Lowe, D. J. *Nature (London)* **1978**, *272*, 557.
(80) Thorneley, R. N. F.; Lowe, D. J. *Biochem. J.* **1984**, *224*, 887.
(81) Davis, L. C. *Arch. Biochem. Biophys.* **1980**, *204*, 270.
(82) Newton, W. E.; Bulen, W. A.; Hadfield, K. L.; Stiefel, E. I.; Watt, G. D. In *Recent Developments in Dinitrogen Fixation*; Newton, W. E., Postgate, J. R., Rodriguez-Barruenco, C., Eds.; Academic Press: New York, 1977; p 119.
(83) Bulen, W. A. *Proc. Int. Symp. Nitrogen Fixation, 1st* **1976**, 177.

NMR operating frequencies and reference standards for heteronuclei on the scale of ^1H (300 MHz, $SiMe_4$ = 0 ppm) are as follows: ^{13}C (75.5 MHz, $SiMe_4$ = 0 ppm), ^{15}N (30.40 MHz, NH_2Ph = 56.5 ppm), and ^{19}F (282.21 MHz, $CFCl_3$ = 0 ppm). Proton and carbon spectra were referenced using the partially deuterated solvent as an internal reference. Other nuclei were referenced externally to the compounds indicated in the same solvent where possible. Chemical shifts are in ppm and coupling constants and line widths are in hertz. All spectra were acquired at room temperature unless otherwise noted. Deuterated solvents were dried by passage through alumina and storage over 4-Å molecular sieves.

IR absorptions are reported in units of cm^{-1}. All spectra were recorded as Nujol mulls between KBr plates, unless otherwise indicated. Solution spectra were recorded using airtight KBr cells. Microanalyses were performed on a Perkin-Elmer PE2400 microanalyzer.

$[Cp^*WMe_4][PF_6]$,[73] $Cp^*WMe_3(OTf)$,[33] $[Cp^*WMe_3(\eta^2\text{-}NHNH_2)]^+$ (**4a**),[42] $[Cp^*WMe_3(\eta^2\text{-}NMeNH_2)]^+$ (**4d**),[42] and $[H(Et_2O)_2][B\{3,5\text{-}(CF_3)_2C_6H_3\}_4]$[84] were prepared according to literature procedures. NH_2NHMe (Aldrich) and NH_2NMe_2 (Aldrich) were distilled from CaH_2 and stored over 4-Å sieves. Hydrazine (Aldrich) was dried over 3-Å sieves. Anhydrous NHMeNHMe was prepared by condensing liquid ammonia (50 mL) onto a mixture of $[NH_2MeNH_2Me]Cl_2$ (Aldrich, 2.94 g, 22.1 mmol) and excess anhydrous Na_2SO_4 at −78 °C. The slurry was slowly warmed to room temperature over 1 h while being stirred vigorously, allowing the ammonia to boil off. Extraction with 20 mL of ether and storage over 4-Å sieves yielded dry NHMeNHMe (1.13 g, 18.8 mmol, 85%) as an ether solution. Methyl triflate, triflic acid anhydride, and triflic acid (Aldrich) were used as purchased.

Preparation of W(V) Hydrazine Adducts (Compounds of Type 1). (a) $[Cp^*WMe_3(\eta^2\text{-}NH_2NH_2)][OTf]$ (1a). Hydrazine (0.075 g, 2.34 mmol, 0.98 equiv) was added to a solution of $Cp^*WMe_3(OTf)$ (1.23 g, 2.36 mmol) in 55 mL of ether at room temperature. After 15 min, orange $[Cp^*WMe_3(\eta^2\text{-}NH_2NH_2)][OTf]$ (1.09 g, 2.00 mmol, 85%) was filtered off and rinsed with ether. Recrystallization from tetrahydrofuran by adding ether and cooling the solution to −40 °C yielded analytically pure orange needles: ESR (THF) $\langle g \rangle$ = 2.012 (47 G); IR (Nujol) 3352 (m, NH_2), 3345 (m, NH_2), 3237 (m, NH_2), 3173 (m, NH_2), 3097 (m, NH_2), 1631 (w, NH_2), 1613 (sh, NH_2), 1601 (w, NH_2), 1574 (w, NH_2). Anal. Calcd for $C_{14}H_{28}F_3N_2O_3SW$: C, 30.84; H, 5.18; N, 5.14. Found: C, 30.49; H, 5.00; N, 4.90.

(b) $[Cp^*WMe_3(\eta^2\text{-}NHMeNHMe)][OTf]$ (1b). A solution of 1,2-dimethylhydrazine (0.049 g, 0.82 mmol, 1.00 equiv) in 3 mL of ether was added to a solution of $Cp^*WMe_3(OTf)$ (0.42 g, 0.82 mmol) in 15 mL of ether at −40 °C. Orange $[Cp^*WMe_3(\eta^2\text{-}NHMeNHMe)][OTf]$ (0.45 g, 0.79 mmol, 96%) precipitated almost immediately. After 15 min, it was filtered off and rinsed with ether. Recrystallization from tetrahydrofuran/ether at −40 °C yielded analytically pure orange-red needles: ESR (THF) $\langle g \rangle$ = 2.004 (22 G); IR (Nujol) 3217 (m, NH), 3144 (m, NH). Anal. Calcd for $C_{16}H_{32}F_3N_2O_3SW$: C, 33.52; H, 5.63; N, 4.89. Found: C, 33.92; H, 5.76; N, 4.78.

(c) Reaction of $Cp^*WMe_3(OTf)$ with PhNHNHPh. See synthesis of $[Cp^*WMe_3(\eta^2\text{-}NPhNHPh)][OTf]$ below.

(d) $[Cp^*WMe_3(\eta^2\text{-}NH_2NHMe)][OTf]$ (1d). A solution of methylhydrazine (0.065 g, 1.39 mmol, 1.05 equiv) in 2 mL of ether was added to a solution of $Cp^*WMe_3(OTf)$ (0.68 g, 1.33 mmol) in 20 mL of ether at room temperature. Orange-red $[Cp^*WMe_3(\eta^2\text{-}NH_2NHMe)][OTf]$ (0.68 g, 1.22 mmol, 92%) precipitated immediately. After 5 min, it was filtered off and rinsed with ether, and recrystallization from tetrahydrofuran/ether at −40 °C yielded analytically pure orange-red needles: ESR (CH_2Cl_2) $\langle g \rangle$ = 2.009 (26 G); IR (Nujol) 3295 (w, NH), 3196 (br, w, NH), 3052 (br, w, NH), 1598 (m, NH_2). Anal. Calcd for $C_{15}H_{30}F_3N_2O_3SW$: C, 32.21; H, 5.41; N, 5.01. Found: C, 32.17; H, 5.65; N, 5.27.

(e) $[Cp^*WMe_3(\eta^2\text{-}NH_2NMe_2)][OTf]$ (1e). 1,1-Dimethylhydrazine (0.059 mL, 0.78 mmol, 1.00 equiv) was added to a solution of $Cp^*WMe_3(OTf)$ (0.40 g, 0.78 mmol) in 30 mL of ether at −40 °C to give an orange precipitate of $[Cp^*WMe_3(\eta^2\text{-}NH_2NMe_2)][OTf]$ (0.34 g, 0.60 mmol, 77%) that was filtered off, rinsed with ether, and dried in vacuo. This compound could not be obtained entirely free of $[Me_2NNH_3][OTf]$: ESR (CH_2Cl_2) $\langle g \rangle$ = 1.992 (22 G); IR (Nujol) 3217 (m, NH), 3144 (m, NH).

Protonation of $[Cp^*WMe_3(\eta^2\text{-}NH_2NH_2)][OTf]$ (1a). A solution of triflic acid (0.053 g, 0.35 mmol, 2.09 equiv) in 2 mL of ether was added to a slurry of $[Cp^*WMe_3(\eta^2\text{-}NH_2NH_2)][OTf]$ (0.092 g, 0.17 mmol) in 10 mL of ether at room temperature. After 10 min, all of the starting material was gone and a fine white precipitate of $[N_2H_6][OTf]_2$ (0.058 g, 0.17 mmol, 100%) had formed and was filtered off. The solvent was removed from the orange filtrate in vacuo to yield $Cp^*WMe_3(OTf)$ (0.084 g, 0.16 mmol, 97%), which was characterized by comparison of its IR spectrum with that of authentic material.[33]

Deprotonation of Hydrazine Adducts $[Cp^*WMe_3(\eta^2\text{-}N_2H_xMe_y)]^+$ (1a, 1b, 1d, 1e; See Table II). Compounds **1** were deprotonated with bases and in solvents listed in Table II, and the ether-soluble products were weighed and analyzed by proton NMR spectra. An example is the following: DBU (0.040 g, 0.26 mmol, 3.97 equiv) in 2 mL of ether was added to a slurry of $[Cp^*WMe_3(\eta^2\text{-}NH_2NHMe)][OTf]$ (0.037 g, 0.066 mmol) in 5 mL of ether. The solution immediately turned yellow. After 10 min the solution was decanted from the insoluble [DBUH][OTf] oil, and the solvent was removed in vacuo. The residue was extracted with ether and dried in vacuo to yield an equimolar mixture of $Cp^*WMe_3(NH)$ and $Cp^*WMe_3(\eta^1\text{-}NNHMe)$.

The diphenylhydrazine adduct **1c** was not observed but was prepared and deprotonated with diphenylhydrazine in situ as described above.

Reduction of Hydrazine Adducts $[Cp^*WMe_3(\eta^2\text{-}N_2H_xMe_y)]^+$ (1a, 1b, 1d, 1e; See Table III). Compounds **1** were reduced in THF or ether by sodium amalgam or sodium naphthalenide to give the products listed in Table III. An example of the reaction is as follows: 0.5% Na/Hg (0.253 g, 0.055 mmol) was added to a 10 mL solution of $[Cp^*WMe_3(\eta^2\text{-}NH_2NH_2)][OTf]$ (0.030 g, 0.055 mmol) at −40 °C in THF. The reaction mixture was stirred vigorously for 30 min, and it changed from an orange solution to a dark yellow-brown solution. The mixture was filtered, and the solvent was removed from the yellow-brown filtrate in vacuo. The residue was extracted with ether to produce a dark yellow-brown solution and a white solid (NaOTf). The solution was filtered, and the solvent was removed from the orange-brown filtrate in vacuo. Proton NMR analysis of the filtrate, using ferrocene as an internal standard, showed it to consist of a mixture of $Cp^*WMe_3(NH)$ and $(Cp^*WMe_3)_2(\mu\text{-}N_2)$ (Table III).

Attempt To Generate $Cp^*WMe_3(NHNH_2)$ (2a) from $Cp^*WMe_3(NH_2)$. Hydrazine (5.0 μL, 0.16 mmol, 1.00 equiv) was added to a solution of $Cp^*WMe_3(NH_2)$[36] (0.060 g, 0.16 mmol) in THF-d_8 in an NMR tube containing ferrocene as an internal standard. Vigorous shaking produced a dark yellow-brown solution. A proton NMR spectrum of the residue obtained upon removing all solvents in vacuo showed it to consist of an equimolar mixture of $Cp^*WMe_3(NH)$ and $Cp^*WMe_3(\eta^1\text{-}NNH_2)$ (88% yield).

Reduction of Compounds 4 (See Table IV). Compounds **4** were reduced in THF by sodium amalgam or sodium naphthalenide to give the products listed in Table IV. The products were quantified by ^1H NMR using ferrocene as an internal standard. An example of a typical reaction is as follows: $[Cp^*WMe_3(\eta^2\text{-}NHNH_2)][OTf]$ (0.100 g, 0.184 mmol) was dissolved in 15 mL of THF at −40 °C. A 1.64 M solution of $Na(C_{10}H_8)$ (0.112 mL, 0.184 mmol) was added directly to the stirring yellow solution. The reaction mixture turned orange immediately and was stirred for 15 min. The solvent was removed in vacuo to produce an orange/red film which was extracted with ether. Filtration produced a white solid and an orange/red filtrate. The solvent was removed from the filtrate in vacuo to give a filmy orange/red solid. The solid was dissolved in CD_2Cl_2 and was a mixture of $Cp^*WMe_3(NH)$, $Cp^*WMe_3(\eta^1\text{-}NNH_2)$, and $[Cp^*WMe_3]_2(\mu\text{-}N_2)$.

Synthesis of $[Cp^*WMe_3(\eta^2\text{-}NMeNHMe)]PF_6$ (4b-PF_6). 1,2-Dimethylhydrazine (1.44 mmol, 1.02 equiv) in ether was added to a slurry of $[Cp^*WMe_4][PF_6]$ (0.74 g, 1.42 mmol) in 20 mL of dichloromethane. The solution immediately turned yellow, and gas evolved vigorously. After 20 min the solution was filtered, and the solvent was removed from the filtrate in vacuo. The product was extracted into tetrahydrofuran, and the product was crystallized at low temperature after addition of ether and then recrystallized in a similar fashion to yield 0.70 g (1.24 mmol, 87%): ^{13}C NMR (CD_2Cl_2) δ 115.96 and 10.60 (Cp^*), 36.99 and 34.97 (WMe_{cis}), 30.75 (WMe_{trans}), 40.45 ($N_\alpha Me$), 32.39 ($N_\beta Me$). Anal. Calcd for $C_{15}H_{31}F_6N_2PW$: C, 31.71; H, 5.50; N, 4.93. Found: C, 31.84; H, 5.44; N, 4.74.

Synthesis of $Cp^*WMe_3(\eta^2\text{-}MeNNMe)$ (5b). A solution of methylmagnesium chloride (0.99 mmol) in 5 mL of THF was added to a solution of $[Cp^*WMe_3(\eta^2\text{-}NMeNMeH)][PF_6]$ (0.560 g, 0.980 mmol) in 40 mL of THF at −40 °C. The reaction mixture changed immediately from yellow to orange-red and gas was evolved. The reaction mixture was stirred for 15 min. The solvent was removed in vacuo to produce an orange-red residue which was extracted with pentane. The extract was filtered, and the orange/red filtrate was concentrated in vacuo to yield crystals of $Cp^*WMe_3(\eta^2\text{-}MeNNMe)$ (0.380 g, 0.900 mmol, 92%): ^1H NMR (C_6D_6, 25 °C) δ 3.01 (br s, 6 H, MeNNMe), 1.41 (s, 15 H, Cp^*), 0.60 (s, 6 H, WMe_{cis}), (0.56, 3 H, WMe_{trans}); ^{13}C NMR (THF-d_8, 20 °C) δ 109.4 (s, C_5Me_5), 39.1 (br q, *Me*NN*Me*), 36.8 (q, WMe_{trans}), 35.8 (q, WMe_{cis}), 9.6 (q, C_5Me_5); IR (Nujol) 1249 (br s, NN), 1226 (sh), 1156 (m), 1032 (m), 837 (w), 643 (m), 518 (w), 488 (m). Anal. Calcd for $WC_{15}H_{30}N_2$: C, 42.67; H, 7.16; N, 6.63. Found: C, 42.87; H, 6.91; N, 6.42.

(84) Brookhart, M.; Grant, B.; Volpe, A. F., Jr. *Organometallics* **1992**, *11*, 3920.

Synthesis of [Cp*WMe$_3$(η^2-NMeNHMe)][OTf] (4b-OTf). A solution of triflic acid (0.041 g, 0.093 mmol, 1.04 equiv) in 2 mL of ether was added to a solution of Cp*WMe$_3$(η^2-MeNNMe) (0.038 g, 0.090 mmol) in 5 mL of ether at −40 °C. A yellow precipitate formed immediately. After 5 min, [Cp*WMe$_3$(η^2-NMeNHMe)][OTf] (0.051 g, 0.089 mmol, 99%) was filtered off and rinsed with ether: ^{1}H NMR (CD_2Cl_2) δ 6.03 (s, 1 H, NH), 3.36 (s, 3 H, NMe), 2.81 (d, $^3J_{HH}$ = 4.8, NH*Me*), 2.00 (s, 15 H, Cp*), 0.50 (s, 3 H, WMe$_{cis}$), 0.44 (s, 3 H, WMe$_{cis}$), 0.30 (s, 3 H, WMe$_{cis}$).

Synthesis of [Cp*WMe$_3$(NMeNMe$_2$)][OTf]. A solution of methyl triflate (0.072 g, 0.44 mmol, 1.11 equiv) in 2 mL of ether was added to a solution of Cp*WMe$_3$(η^2-MeNNMe) (0.167 g, 0.40 mmol) in 5 mL of ether at −40 °C. The color of the solution slowly changed from red-orange to yellow while a light-yellow precipitate slowly formed; after 15 min, pale-yellow, crystalline [Cp*WMe$_3$(η^2-NMeNMe$_2$)][OTf] (0.057 g, 0.097 mmol, 82%) was filtered off and recrystallized from dichloromethane/ether: ^{1}H NMR (CD_2Cl_2) δ 3.36 (N$_\alpha$Me), 2.82 (N$_\beta$Me), 2.03 (Cp*), 0.59 (WMe$_{cis}$), 0.48 (WMe$_{trans}$); ^{13}C NMR (CD_2Cl_2) δ 115.25 and 10.19 (Cp*), 39.23 (WMe$_{cis}$), 32.80 (WMe$_{trans}$), 36.86 (N$_\alpha$Me), 45.09 (N$_\beta$Me). Anal. Calcd for $C_{17}H_{33}F_3O_3N_2SW$: C, 34.82; H, 5.67; N, 4.78. Found: C, 35.04; H, 5.77; N, 5.00.

Synthesis of Cp*WMe$_3$(η^2-PhNNPh) (5c). An excess of NaH was added to a slurry of [Cp*WMe$_3$(η^2-NPhNHPh)][OTf] (108 mg, 0.155 mmol) in 6 mL of THF. The red reaction mixture was stirred for 15 min, and then it was filtered. The THF was removed from the filtrate in vacuo, and the residue was extracted with pentane. Practically pure dark red crystalline **5c** was obtained upon removing the pentane in vacuo (80 mg, 94%). An analytically pure sample was obtained by recrystallization from cold pentane: ^{1}H NMR (C_6D_6) δ 7.33 (d, 2), 7.17 (t, 2), 6.85 (t, 1), 1.46 (s, 15), 0.85 (s, 3), 0.8 (v br, 3); ^{13}C NMR (C_6D_6) δ 153.0 (arom C), 128.3, 123.0, 121.8 (arom *C*H), 110.07 (Cp**C*), 42.5 (W*C*H$_3$), 9.77 (Cp**C*H$_3$). Anal. Calcd for $WC_{25}H_{34}N_2$: C, 54.99; H, 6.27; N, 5.13. Found: C, 54.66; H, 6.36; N, 4.95.

Synthesis of [Cp*WMe$_3$(η^2-PhNNHPh)][OTf] (4c). A solution of diphenylhydrazine (362 mg, 1.96 mmol, 0.99 equiv) in 10 mL of ether was added to Cp*WMe$_3$(OTf) (1.02 g, 1.99 mmol) partially dissolved in 50 mL of ether at room temperature. The reaction mixture was stirred for 3 days, during which time a yellow solid precipitated out of solution (90% in the first 24 h).

The precipitate was extracted with methylene chloride; anilinium triflate was left behind (175 mg, 73%). The methylene chloride was removed from the extract in vacuo to give [Cp*WMe$_3$(η^2-NPhNHPh)][OTf] (574 mg, 84% crude yield). The product was recrystallized twice from dichloromethane (by adding ether and cooling to −40 °C) to afford analytically pure yellow needles: ^{1}H NMR (CD_2Cl_2) δ 8.80 (s, 1 H, N*H*), 7.52–7.06 (m, 10 H, arom *H*), 1.99 (s, 15 H, Cp*), 0.99 (s, 3 H, trans Me), 0.52 (s, 3 H, cis methyl), 0.46 (s, 3 H, cis methyl); ^{19}F NMR δ −78.01; IR (Nujol mull, KBr) 3350 (w, NH), 3142 (NH), 1595 (m, NH). Anal. Calcd for $WC_{26}H_{35}F_3N_2O_3S$: C, 44.83; H, 5.03; N, 4.03. Found: C, 44.88; H, 5.08; N, 4.00.

The ether solvent was removed from the mother liquor, and the residue was extracted with pentane. The pentane was removed in vacuo to give Cp*WMe$_3$(NPh) (333 mg, 73% crude yield). This compound was identified by IR and NMR comparison with an authentic sample.[36]

[Cp*WMe$_3$(η^2-PhNNHPh)][OTf] also can be prepared from **5c** in ether at −40 °C by adding 1 equiv of triflic acid (in ether); filtration of the reaction mixture gives **4c** quantitatively. Protonation of **5c** by lutidinium triflate under similar conditions is slow, the time required being proportional to the scale of the reaction.

Reduction of Cp*WMe$_3$(η^2-PhNNPh). A solution of Cp*WMe$_3$(η^2-PhNNPh) (32 mg, 0.46 mmol) in 4 mL of C_6D_6 was added to Na/Hg (2.0 g, 0.5%, excess), and the reaction mixture was stirred at room temperature for 16 h. A proton NMR spectrum of the red reaction mixture showed Cp*WMe$_3$(NPh) as the only observable product. Removing the solvent in vacuo afforded **5c** in 65% yield.

Stoichiometric Generation of Ammonia. Method 1. Under an atmosphere of N_2, 30 mg of each of the metal complexes under study (Cp*WMe$_3$(η^1-NNH$_2$) and [Cp*WMe$_3$(η^2-NH$_2$NH$_2$)]$^+$) were weighed out into a 50-mL Schlenk flask. Reductant and proton source were added to the flask (6 and 12 equiv, respectively, for the Cp*WMe$_3$(η^1-NNH$_2$); 4 and 8 equiv, respectively, for [Cp*WMe$_3$(η^2-NH$_2$NH$_2$)]$^+$, which was then capped with a septum and wired shut. Cold (−40 °C) THF (10 mL) was added to the flask via syringe, and the reaction mixture was stirred vigorously. The reaction mixtures slowly changed color to form a gray-green solid in a dark brown solution. After the solution was allowed to stand ~20 h at 25 °C, 100 μL of concentrated HCl was added to the reaction mixture by syringe to react with any remaining NH_3. The solvent was then immediately removed in vacuo, and the residue was treated with 15 mL of a 4.0 M NaOH solution in a closed system under argon. The basic solution was then gently distilled into 15 mL of 0.5 N H_2SO_4 until ~10–15 mL of the distillate had been collected. The volume of the acid solution was then brought up to 30 mL with distilled water. This solution was tested quantitatively for ammonia using the indophenol test.[85]

Method 2. This method only differs from method 1 in the workup of the reaction mixture. After the solution was allowed to stand ~20 h at 25 °C, 100 μL of concentrated HCl was added to the reaction mixture by syringe. The solvent was then immediately removed in vacuo. The remaining solids were then extracted with 30 mL of distilled H_2O, which was then passed through a Millipore filter to remove the insoluble solids. Aliquots of this solution, diluted if necessary, were tested quantitatively for ammonia by using the indophenol test.[85] The yields of NH_3 from this method varied only slightly (±3%) from the data obtained by method 1.

Catalytic Reduction of Hydrazine to Ammonia. Under an atmosphere of N_2, 30 mg of the metal complex being studied (Cp*WMe$_3$(η^1-NNH$_2$) or [Cp*WMe$_3$(η^2-NH$_2$NH$_2$)]$^+$), 16 equiv of lutidine·HCl (or phenol), and 12 equiv of 87% Zn/Hg were weighed out into a 50-mL Schlenk flask, which was then capped with a septum and wired shut. Cold (−40 °C) THF (10 mL) was added to the flask via syringe followed by the required amount of N_2H_4, and the reaction mixture was stirred vigorously. The reaction mixtures slowly changed color to form a gray/green solid in a dark brown solution. After the solution was allowed to stand for 20–28 h (dependent on the concentration of hydrazine) at 25 °C, 200 μL of concentrated HCl was added to the reaction mixture by syringe to react with any remaining NH_3. The solvent was then immediately removed in vacuo, and the residue was either treated with 4.0 M NaOH followed by base distillation as described above in method 1 of the stoichiometric reduction studies or was extracted with H_2O as described in method 2. Samples from the solutions were then taken and tested for ammonia by the indophenol test.[85]

X-ray Crystal Structure of [Cp*WMe$_3$(η^2-NH$_2$NH$_2$)][OTf] (1a). An off-white crystal of **1a** (0.28 × 0.28 × 0.18 mm, obtained from dichloromethane) was mounted on a glass fiber. Data were collected at −78 °C on a Rigaku AFC6R diffractometer with graphite monochromated Mo Kα radiation (λ = 0.71069 Å). A total of 4362 reflections were collected in the range of 3.00° < 2θ < 50.00°, with 4261 being unique. No crystal decay was evident during the data collection. An empirical absorption correction was applied using the program DIFABS which resulted in transmission factors ranging from 0.83 to 1.36. The structure was solved using the direct methods. The non-hydrogen atoms were refined anisotropically. Hydrogen atoms were included in the structure factor calculation in idealized positions. The final cycle of full-matrix least-squares refinement was based on 2933 reflections (I > 3.00$\sigma(I)$) and 307 variables and used the TEXSAN crystallographic software package from Molecular Structure Corporation. The final refinement converged with final R = 0.034 and R_w = 0.044. The maximum and minimum peaks on the final Fourier difference map corresponded to 0.97 and −0.87 e$^-$/Å^3, respectively. Crystal data are as follows: space group = $C2/c$ (No. 15), a = 32.60(1) Å, b = 8.587(3) Å, c = 22.68(1) Å, β = 121.25(3)°, V = 5427(4) Å^3, MW = 689.51, ρ (calcd) = 1.688 g/cm^3, Z = 8, R = 0.034, R_w = 0.044, μ = 44.7 cm^{-1}.

X-ray Crystal Structure of Cp*WMe$_3$(η^2-MeNNMe) (5b). An orange prismatic crystal of $WC_{15}H_{30}N_2$ having approximate dimensions of 0.20 × 0.20 × 0.16 mm was mounted on a glass fiber. Data were collected at −72 °C on an Enraf–Nonius CAD-4 diffractometer with graphite monochromated Mo Kα radiation. A total of 4060 reflections were collected in the range 3.0° < 2θ < 55.00°, with 3835 being unique. No crystal decay was evident during data collection. An empirical absorption correction was applied using the program DIFABS which resulted in transmission factors ranging from 0.87 to 1.28. The structure was solved by Patterson methods. The non-hydrogen atoms were refined anisotropically. Hydrogen atoms were included in the structure factor calculation in idealized positions and refined isotropically. The final cycle of full-matrix least-squares refinement was based on 2700 reflections (I > 3.00$\sigma(I)$) and 164 variables and used the TEXSAN crystallographic software package from Molecular Structure Corporation. The final refinement converged with final R = 0.040 and R_w = 0.041. The maximum and minimum peaks on the final Fourier difference map corresponded to 1.10 and −1.40 e$^-$/Å^3, respectively. Crystal data are as follows: a = 9.392(4) Å, b = 11.721(5) Å, c = 14.520(4) Å, β = 93.67(3)°, V = 1595(3) Å^3, space group = $P2_1/a$, Z = 4, MW = 422.27, ρ (calcd) = 1.761 g/cm^3, μ = 41.62 cm^{-1}.

Acknowledgment. R.R.S. thanks the National Institutes of Health for support (Grant GM 31978), and T.E.G. and M.G.V. thank the National Science Foundation for predoctoral fellowships.

(85) Chaney, A. L.; Marbach, E. P. *Clin. Chem.* **1962**, *8*, 130.

We all thank Dr. W. M. Davis for collecting X-ray data and Prof. M. Brookhart for providing details of the synthesis of $[H(Et_2O)_2][B\{3,5\text{-}(CF_3)_2C_6H_3\}_4]$ prior to publication.

Supplementary Material Available: Experimental details of X-ray study, labeled ORTEP drawing, final positional parameters, and final thermal parameters for **1a** (6 pages); final observed and calculated structure factors for **1a** (21 pages). Supplementary material for **5b** is available elsewhere.[37] Ordering information is given on any current masthead page.

Reevaluation of the Significance of ^{18}O Incorporation in Metal Complex-Catalyzed Oxygenation Reactions Carried Out in the Presence of $H_2{}^{18}O$

Wonwoo Nam[†] and Joan Selverstone Valentine*,[‡]

Contribution from the Department of Chemistry and Biochemistry, University of California, Los Angeles, California 90024, and Department of Science, Hong Ik University, 72-1 Sangsudong, Mapogu, Seoul, Korea. *Received September 14, 1992*

Abstract: We have measured the extent of ^{18}O incorporation into the products of metal complex-catalyzed oxygenations of organic compounds when $H_2{}^{18}O$ is added to the reaction mixture. The oxidants studied were hydrogen peroxide, *tert*-butyl hydroperoxide, *m*-chloroperbenzoic acid (MCPBA), and iodosylbenzene, and the reactions were carried out in organic solvents. In reactions of hydrogen peroxide, *tert*-butyl hydroperoxide, and MCPBA, no or at most a small amount of ^{18}O was incorporated into the products in either olefin epoxidation or alkane hydroxylation reactions catalyzed by (*meso*-tetrakis(2,6-dichlorophenyl)porphinato)iron(III) chloride (Fe(TDCPP)Cl), (*meso*-tetrakis(2,6-dichlorophenyl)porphinato)manganese(III) chloride (Mn(TDCPP)Cl) with imidazole added, iron(II) cyclam (cyclam = 1,4,8,11-tetraazacyclotetradecane), manganese(II) cyclam, and nickel(II) cyclam. Assuming that high-valent metal oxo intermediates are generated in all of the reactions of iron and manganese porphyrin complexes with the oxidants PhIO, H_2O_2, *tert*-butyl hydroperoxide, and MCPBA, we conclude that the high-valent iron oxo and manganese oxo intermediates do not exchange or slowly exchange with labeled $H_2{}^{18}O$ during the course of these catalytic oxygenation reactions under our reaction conditions. Several different iron(III) and manganese(III) porphyrin complexes such as Fe(TDCPP)Cl, (*meso*-tetraphenylporphinato)iron(III) chloride (Fe(TPP)Cl), (*meso*-tetramesitylporphinato)iron(III) chloride (Fe(TMP)Cl), and Mn(TDCPP)Cl were used to catalyze cyclohexene epoxidation by MCPBA at low temperature (−78 °C) in the presence of $H_2{}^{18}O$. The epoxide obtained in the epoxidation of cyclohexene catalyzed by Fe(TDCPP)Cl, Fe(TPP)Cl, Fe(TMP)Cl, and Mn(TDCPP)Cl contained 0%, 4%, 22%, and 0% ^{18}O, respectively. By contrast, in the iodosylbenzene reactions, oxygen from labeled $H_2{}^{18}O$ was fully incorporated into products in aprotic and protic solvents in olefin epoxidation and alkane hydroxylation reactions catalyzed by either iron(III) porphyrin, manganese(III) porphyrin, or metallocyclam (M = Fe, Mn, Ni) complexes. Labeled oxygen from $H_2{}^{18}O$ was also fully incorporated into cyclohexene oxide in the epoxidation of cyclohexene catalyzed by a zinc complex which is not able to form a high-valent zinc oxo species as an intermediate. We conclude from these results that, in the case of iodosylbenzene, the mechanism for oxygen exchange does not involve metal oxo intermediates and that the observation of incorporation of labeled oxygen from $H_2{}^{18}O$ into products does not provide evidence for the intermediacy of metal oxo complexes in iodosylbenzene reactions. In the case of oxidants other than iodosylbenzene, our results also suggest that reactions of high-valent metal oxo complexes with organic substrates in catalytic oxygenation reactions are often comparable in rate to or faster than the reactions with isotopically labeled water that lead to oxygen exchange.

Introduction

Elucidation of the mechanism of oxygen atom-transfer reactions by monooxygenase enzymes has been a major goal of biological and bioinorganic chemistry.[1] Intensive study of cytochrome P-450 and its model compounds such as metalloporphyrins has resulted in a proposed catalytic cycle which involves a high-valent iron oxo species as the oxygenating agent.[1c,d,2] Although high-valent iron oxo species have been widely proposed as the oxygenating intermediates in the catalytic cycle of heme and non-heme iron-containing monooxygenase enzymes and their model compounds, direct evidence for the high-valent iron oxo species has frequently been difficult to obtain.

Several reports have appeared suggesting that high-valent metal oxo complexes exchange oxygen atoms rapidly with $H_2{}^{18}O$ when labeled water is added to such complexes after they have been generated in organic solvents. Thus, it has been found that (1) the oxygen atom in $Cr^V(TPP)(O)Cl$ exchanged with the labeled oxygen of $H_2{}^{18}O$,[3a] (2) $(TMP)^{\bullet+}Fe^{IV}(O)Cl$, generated in situ from the reaction of Fe(TMP)Cl and MCPBA at −78 °C, epoxidized norbornene in the presence of $H_2{}^{18}O$, resulting in the formation

Scheme I

$$LM^{n+} + X^{16}O \xrightarrow{-X} [LM^{(n+2)+}{=}{}^{16}O]$$

$$[LM^{(n+2)+}{=}{}^{16}O] \xrightarrow[\text{fast}]{H_2{}^{18}O} [LM^{(n+2)+}{=}{}^{18}O]$$

$$[LM^{(n+2)+}{=}{}^{18}O] \xrightarrow{S} S(^{18}O) + LM^{n+}$$

(S = substrate)

[†] Hong Ik University.
[‡] University of California, Los Angeles.

(1) (a) Dix, T. A.; Benkovic, S. J. *Acc. Chem. Res.* **1988**, *21*, 101. (b) Walsh, C.; Chen, Y.-C. J. *Angew. Chem., Int. Ed. Engl.* **1988**, *27*, 333. (c) Guengerich, F. P.; Macdonald, T. L. *Acc. Chem. Res.* **1984**, *17*, 9. (d) White, R. E.; Coon, N. J. *Annu. Rev. Biochem.* **1980**, *49*, 315. (e) Ullrich, V. *Angew. Chem., Int. Ed. Engl.* **1972**, *11*, 701.

(2) (a) Ortiz de Montellano, P. R., Ed. *Cytochrome P-450: Structure, Mechanism, and Biochemistry*; Plenum: New York, 1985. (b) White, W. *Bioorg. Chem.* **1990**, *18*, 440. (c) Tabushi, I. *Coord. Chem. Rev.* **1988**, *86*, 1. (d) Mansuy, D. *Pure Appl. Chem.* **1987**, *59*, 759.

0002-7863/93/1515-1772$04.00/0